Supporting Experimental Information

From Organotin Hydrides to Heteronuclear Main Group Metal Compounds: Isolation of the first neutral Bismuth/Tin Clusters

Beate G. Steller, Michaela Flock and Roland C. Fischer*
Institute of Inorganic Chemistry, Graz University of Technology, Stremayrgasse 9/V, 8010 Graz, AUSTRIA

Table of Contents

1 Supplementary graphs and tables

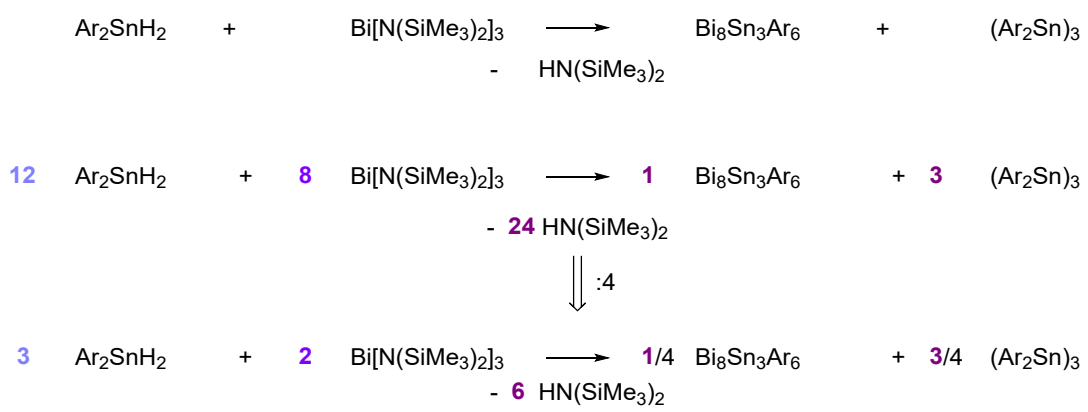

Scheme S 1 Putative stoichiometry for formation of **1** and **4**.

Table S 1 Selected average bond lengths [Å] and angles [°] of mixed bismuth/tin compounds **1**, **3**, **4**, **6** and **7**.

	Space group	**Bi-Sn** [Å] (avg.)	**Bi-Bi** [Å] (avg.)	**Bi-Sn-Bi** [°] (avg.)	**Bi-Bi-Bi** [°] (avg.)
$Bi_8Sn_3Tripp_6$ (**1**)	$P\bar{1}$	2.9162(1)	3.0005(7)	107.05(6)	104.43(4)
$Bi_4Sn_4H_2Tripp_8$ (**3**)	$P\bar{1}$	2.9046(8)	3.0105(1)	88.85(8)	85.69(7)
$Bi_8Sn_3Dipp_6$ (**4**)	C2/c	2.9060(6)	2.9826(8)	106.78(5)	104.34(1)
$Bi_4Sn_4H_2Dipp_8$ (**6**)	$P\bar{1}$	2.9084(5)	2.0085(2)	91.72(7)	87.99(6)
$Bi_2Sn_4Dipp_6$ (**7**)	$P4_1$	2.937(8)	-	87.92(6)	-

2 Experimental Details

General

All manipulations involving air or moisture sensitive compounds were either performed under a nitrogen atmosphere using standard Schlenk tube techniques or were carried out in a nitrogen flushed Glovebox UNILAB supplied by M.Braun. Anhydrous and deoxygenated solvents were obtained from an Innovative Technology solvent drying system. Compounds $Tripp_2SnH_2$, $Dipp_2SnH_2$ and $Bi[N(SiMe_3)_2]_3$ were prepared according to literature procedures.[1,2] All other chemicals from commercial sources were used as purchased from chemical suppliers. Elemental analysis was performed with an Elementar Vario MICRO cube. Melting points were determined by threefold determination with an electrothermal Mel-Temp instrument.

Synthesis of $Bi_8Sn_3Tripp_6$ (1)

A solution of 460 mg $Bi[N(SiMe_3)_2]_3$ (0.67 mmol, 2.0 eq) in 4 mL DME was added dropwise to 528 mg $Tripp_2SnH_2$ (1.0 mmol, 3.0 eq) also dissolved in 4 mL DME. The solution turned briefly red but slowly faded to reddish brown. After 6 days concentration of the reaction mixture to about 2 mL gave **1** as dark brownish red rods suitable for single crystal X-ray diffraction. The supernatant solution was stored at -30°C to give greenish-yellow blocks of *cyclo*-$(Tripp_2Sn)_3$ (**2**) as a byproduct.

Analytical data for $Bi_8Sn_3Tripp_6$ (**1**):

Yield: 144 mg (13% yield referred to $Tripp_2SnH_2$, 53% yield referred to $Bi[N(SiMe_3)_2]_3$), brownish red needles. m.p.^{exp} >150°C (decomp.). Anal. Calcd. for $C_{98}H_{158}Bi_8O_4Sn_3$ ($Bi_8Sn_3Tripp_6$*2 DME): C, 34.33; H, 4.65. Found: C, 36.84; H, 4.70.

^{1}H NMR (300.22 MHz, d_8-THF, -10°C) δ 7.02 (s, 6 H; 6xH^{Ar}), 6.73 (s, 6 H; 6xH^{Ar}), 3.83-3.79 (m, 6 H; 6x*o*-C*H*$(CH_3)_2$), 2.72 (sept, $^3J_{H,H}$ = 6.9 Hz, 6 H, 6x*p*-C*H*$(CH_3)_2$), 2.63-2.59 (m, 6 H; 6x*o*-C*H*$(CH_3)_2$), 1.67 (d, $^3J_{H,H}$ = 6.9 Hz, 18 H; 3x*o*-CH(C*H*$_3)_2$, overlay with solvent peak), 1.33 (d, $^3J_{H,H}$ = 6.5 Hz, 18 H; 3x*o*-CH(C*H*$_3)_2$), 1.14-1.11 (m, 36 H, 6x*p*-CH(C*H*$_3)_2$), 1.08 (d, $^3J_{H,H}$ = 6.5 Hz, 18 H; 3x*o*-CH(C*H*$_3)_2$), 0.12 (d, $^3J_{H,H}$ = 5.6 Hz, 18 H; 3x*o*-CH(C*H*$_3)_2$) ppm. ^{13}C NMR (75.5 MHz, d_8-THF, -10°C) δ 154.30 (C^{Ar}), 153.7 (C^{Ar}), 153.6 (C^{Ar}), 149.8 (C^{Ar}), 124.4 (C^{Ar}), 124.1 (C^{Ar}), 40.6 (*C*H$(CH_3)_2$), 37.0 (*C*H$(CH_3)_2$), 35.4 (CH(*C*H$_3)_2$), 33.6 (*C*H$(CH_3)_2$), 28.1 (CH(*C*H$_3)_2$), 27.2 (CH(*C*H$_3)_2$), 24.6 (CH(*C*H$_3)_2$), 24.5 (CH(*C*H$_3)_2$), 22.2 (CH(*C*H$_3)_2$) ppm. ^{119}Sn NMR (111.92 MHz, C_6D_6) δ -927.3 (broad, $Tripp_2$*Sn*) ppm. ^{119}Sn NMR (111.92 MHz, d_8-THF) δ -924.8 (broad, $Tripp_2$*Sn*) ppm. UV-Vis (THF) λ_{max} (ε, L cm^{-1}mol^{-1}) 657 (1862), 576 (6615), 488 (12201), 438 (14326), 378 (-), 308 (-) nm. Raman (140 mW, 10 scans) 268 (14), 456 (8), 552 (17), 597 (33), 742 (15), 835 (15), 880 (22), 956 (12, (1101 (26), 1256 (69), 1346 (100), 1593 (37), 1679 (49), 1907 (41) cm^{-1}.

Analytical data for *cyclo*-$(Tripp_2Sn)_3$ (**2**) agree with literature values:[3]

^{1}H NMR (300.22 MHz, C_6D_6) δ 7.11 (s, 6 H; 6xH^{Ar}), 7.06 (s, 6 H; H^{Ar}), 3.36 (m, 12 H; *o*-C*H*$(CH_3)_2$), 2.80 (sept, $^3J_{H,H}$ = 6.8 Hz, 6 H; *o*-C*H*$(CH_3)_2$), 1.50 (d, $^3J_{H,H}$ = 6.6 Hz, 18 H; 3xCH(C*H*$_3)_2$), 1.33-1.19 (m, 54 H; 9xCH(C*H*$_3)_2$), 0.81 (d, $^3J_{H,H}$ = 6.5 Hz, 18 H; 3xCH(C*H*$_3)_2$), 0.62 (d, $^3J_{H,H}$ = 6.3 Hz, 18 H, 3xCH(C*H*$_3)_2$) ppm.

^{13}C NMR (75.5 MHz, C_6D_6) δ 155.0 (C^{Ar}), 154.8 (C^{Ar}), 149.6 (C^{Ar}), 143.5 (C^{Ar}), 122.7 (C^{Ar}), 122.4 (C^{Ar}), 122.0 (C^{Ar}), 40.5 (*C*H$(CH_3)_2$), 39.1 (*C*H$(CH_3)_2$), 34.8 (*C*H$(CH_3)_2$), 34.6 (*C*H$(CH_3)_2$), 27.3 (CH(*C*H$_3)_2$), 26.8 (CH(*C*H$_3)_2$), 26.2 (CH(*C*H$_3)_2$), 25.4 (CH(*C*H$_3)_2$), 24.5 (CH(*C*H$_3)_2$), 24.4 (CH(*C*H$_3)_2$), 24.3 (CH(*C*H$_3)_2$) ppm. ^{119}Sn NMR (111.92 MHz, C_6D_6) δ -371.3 ($^1J_{Sn,117Sn}$ = 3048 Hz) ppm.

Synthesis of $Bi_4Sn_4H_2Tripp_8$ (3)

A solution of 460 mg $Bi[N(SiMe_3)_2]_3$ (0.67 mmol, 2.0 eq) in 3 mL DME was added dropwise to 528 mg $Tripp_2SnH_2$ (1.0 mmol, 3.0 eq) also dissolved in 2 mL DME. The solution turned briefly red but slowly faded to reddish brown. After 2 days the product crystallized from the dark brownish red solution as red-brown rhombic plates, which turned out to be suitable for single crystal X-ray diffraction. The supernatant solution was concentrated and stored at -30°C to give *cyclo*-$(Tripp_2Sn)_3$ as a byproduct.

Note: Prolonged standing (> 6 days) of the reaction mixture at room temperature resulted in complete consumption of initially precipitated **3**, whereupon crystals of **1** were formed. Upon concentration of the mother liquor, an additional batch of **1** together with yellow crystals of **2** was isolated.

Analytical data for $Bi_4Sn_4Tripp_6H_2$ **(3)**:

Yield: 35 mg (1% yield referred to $Tripp_2SnH_2$, 2% yield referred to $Bi[N(SiMe_3)_2]_3$), redbrown rhombic plates. m.p.^{exp} >121°C (decomp.). Anal. Calcd. for $C_{120}H_{186}Bi_4Sn_4$ ($Bi_4Sn_4Tripp_6H_2$): C, 49.03; H, 6.38. Found: C, 49.23; H, 6.47.

^{1}H NMR (300.22 MHz, C_6D_6) δ 9.68 (s, 2 H; 2xSn*H*), 7.26 (s, 4 H; 4xH^{Ar}), 7.10 (s, 4 H; 4xH^{Ar}), 6.78 (s, 4 H; 4xH^{Ar}), 6.42 (s, 4 H; 4xH^{Ar}), 4.90-4.86 (m, 4 H; 4x*o*-C*H*$(CH_3)_2$), 4.70-4.66 (m, 4 H; 4x*o*-C*H*$(CH_3)_2$), 2.82-2.63 (m, 12 H; 8xp-C*H*$(CH_3)_2$ and 4x*o*-C*H*$(CH_3)_2$, overlay with TrippH and *cyclo*-$(Tripp_2Sn)_3$), 2.55-2.51 (m, 4 H; 4x*o*-C*H*$(CH_3)_2$), 2.32 (d, $^3J_{H,H}$ = 6.6 Hz, 12 H; 2xCH(C*H*$_3)_2$), 2.09 (d, $^3J_{H,H}$ = 6.6 Hz, 12 H; 2xCH(C*H*$_3)_2$), 1.72-1.66 (m, 24 H; 4xCH(C*H*$_3)_2$),1.50 (d, $^3J_{H,H}$ = 6.4 Hz, 24 H; 2xCH(C*H*$_3)_2$), 0.96 (d, $^3J_{H,H}$ = 6.5 Hz, 12 H; 2xCH(C*H*$_3)_2$), 0.80 (d, $^3J_{H,H}$ = 6.4 Hz, 24 H; 2xCH(C*H*$_3)_2$), 0.62 (d, $^3J_{H,H}$ = 6.4 Hz, 24 H; 2xCH(C*H*$_3)_2$), 0.26 (d, $^3J_{H,H}$ = 6.7 Hz, 12 H; 2xCH(C*H*$_3)_2$) ppm.

^{13}C NMR (75.5 MHz, C_6D_6) δ 157.2 (C^{Ar}), 155.8 (C^{Ar}), 155.6 (C^{Ar}), 155.4 (C^{Ar}), 155.0 (C^{Ar}), 155.0 (C^{Ar}), 154.9 (C^{Ar}), 153.5 (C^{Ar}), 149.9 (C^{Ar}), 149.6 (C^{Ar}), 149.4 (C^{Ar}), 149.2 (C^{Ar}), 144.0 (C^{Ar}), 143.6 (C^{Ar}), 136.9 (C^{Ar}), 122.7 (C^{Ar}), 122.2 (C^{Ar}), 122.0 (C^{Ar}), 121.9 (C^{Ar}), 120.5 (C^{Ar}), 120.3 (C^{Ar}), 120.2 (C^{Ar}), 119.2 (C^{Ar}), 112.4 (C^{Ar}), 44.0 (*C*H$(CH_3)_2$), 40.8 (*C*H$(CH_3)_2$), 40.5 (*C*H$(CH_3)_2$), 39.9 (*C*H$(CH_3)_2$), 39.1 (*C*H$(CH_3)_2$), 34.6 (*C*H$(CH_3)_2$), 34.6 (CH(*C*H$_3)_2$), 34.5 (*C*H$(CH_3)_2$), 34.4 (CH(*C*H$_3)_2$), 30.6 (*C*H$(CH_3)_2$), 28.7 (*C*H$(CH_3)_2$), 27.3 (CH(*C*H$_3)_2$), 26.8 (CH(*C*H$_3)_2$), 26.2 (*C*H$(CH_3)_2$), 26.2 (CH(*C*H$_3)_2$), 25.8 (*C*H$(CH_3)_2$), 25.7 (*C*H$(CH_3)_2$), 25.4 (CH(*C*H$_3)_2$), 25.2 (CH(*C*H$_3)_2$), 24.9 (CH(*C*H$_3)_2$), 24.6 (CH(*C*H$_3)_2$), 24.6 (CH(*C*H$_3)_2$), 24.5 (CH(*C*H$_3)_2$), 24.4 (CH(*C*H$_3)_2$), 24.4 (CH(*C*H$_3)_2$), 24.3 (CH(*C*H$_3)_2$), 24.3 (CH(*C*H$_3)_2$), 24.2 (CH(*C*H$_3)_2$), 23.4 (CH(*C*H$_3)_2$) ppm.

ATR-FTIR $\tilde{\nu}$ 3040 (w), 2952 (s), 2870 (m), 1794 (m), 1554 (m), 1458 (s), 1379 (m), 1233 (w), 1097 (m), 874 (s), 741 (m), 562 (m), 389 (s) cm^{-1}.

UV-vis (benzene) λ_{max} (ε, L cm^{-1}mol^{-1}) 844 (268), 658 (218), 565 (-), 497 (5229), 390 (-) nm.

Synthesis of $Bi_4Sn_4H_2Dipp_6$ (6)

A solution of 460 mg $Bi[N(SiMe_3)_2]_3$ (0.67 mmol, 2.0 eq) in 4 mL DME was added dropwise to 443 mg $Dipp_2SnH_2$ (1.0 mmol, 3.0 eq) also dissolved in 4 mL DME. The solution turned briefly red and but slowly faded to reddish brown. After 2 days the product crystallized from the dark brownish red solution as red-brown rhombic plates suitable for single crystal X-ray diffraction. The supernatant solution was concentrated and stored at -30°C to give *cyclo*-$(Dipp_2Sn)_3$ as a byproduct. Note: When the crystalline precipitate of **6** was not isolated after 48 hours but left in contact with the supernatant, the crystals of **6** were slowly consumed. The conversion of **6** completed after 6-9 days to yield a dark red reaction mixture from which a mixture of **4** and **5** precipitated. These were separated by recrystallization from *n*-pentane.

Analytical data for $Bi_4Sn_4H_2Dipp_6$ (**6**):

Yield: 23 mg (4% yield referred to $Dipp_2SnH_2$, 5% yield referred to $Bi[N(SiMe_3)_2)_3]$, redbrown rhombic plates. m.p.^{exp} >104°C (decomp.). Anal. Calcd. for $C_{96}H_{148}Bi_4O_2Sn_4$ ($Bi_4Sn_4Dipp_6H_2$* DME): C, 43.76; H, 5.28. Found: C, 44.02; H, 5.37.

^{1}H NMR (300.22 MHz, C_6D_6) δ 9.60 (s, 2 H; 2xSn*H*), 7.07–6.87 (m, 16 H; 8x*p*-H^{Ar} and 8x*m*-H^{Ar}), 6.79 (d, $^3J_{H,H}$ = 7.4 Hz, 4 H; 4x*m*-H^{Ar}), 6.39 (d, $^3J_{H,H}$ = 7.2 Hz, 4 H; 4x*m*-H^{Ar}), 4.86-4.77 (m, 4 H; 4xC*H*$(CH_3)_2$), 4.56-4.47 (m, 4 H; 4xC*H*$(CH_3)_2$), 2.81-2.72 (m, 4 H; 4xC*H*$(CH_3)_2$), 2.48-2.40 (m, 4 H; 4xC*H*$(CH_3)_2$), 2.23 (d, $^3J_{H,H}$ = 6.7 Hz, 12 H; 2xCH(C*H*$_3)_2$), 2.00 (d, $^3J_{H,H}$ = 6.8 Hz, 12 H; 2xCH(C*H*$_3)_2$), 1.61-1.55 (m, 24 H; 4xCH(C*H*$_3)_2$), 0.93 (d, $^3J_{H,H}$ = 6.5 Hz, 12 H; 2xCH(C*H*$_3)_2$), 0.57-0.53 (m, 24 H; 2xCH(C*H*$_3)_2$), 0.13 (d, $^3J_{H,H}$ = 6.6 Hz, 12 H; 2xCH(C*H*$_3)_2$) ppm. ^{1}H NMR (300.22 MHz, d_8-THF) δ 9.29 (s, 2 H; 2xSn*H*), 7.28 (d, $^3J_{H,H}$ = 7.6 Hz, 4 H; 4x*m*-H^{Ar}), 7.12-7.07 (m, 8 H; 4x*m*-H^{Ar}), 7.00 (d, $^3J_{H,H}$ = 7.6 Hz, 4 H; 4x*m*-H^{Ar}), 6.80 (d, $^3J_{H,H}$ = 7.6 Hz, 4 H; 4x*m*-H^{Ar}), 6.38-6.35 (m, 4 H; 4x*m*-H^{Ar}), 4.67-4.58 (m, 4 H; 4xC*H*$(CH_3)_2$), 4.39-4.29 (m, 4 H; 4xC*H*$(CH_3)_2$), 2.62-2.54 (m, 4 H; 4xC*H*$(CH_3)_2$), 2.28-2.20 (m, 4 H; 4xC*H*$(CH_3)_2$), 2.10 (d, $^3J_{H,H}$ = 6.7 Hz, 12 H; 2xCH(C*H*$_3)_2$), 1.87 (d, $^3J_{H,H}$ = 6.8 Hz, 12 H; 2xCH(C*H*$_3)_2$), 1.52-1.42 (m, 24 H; 4xCH(C*H*$_3)_2$), 0.77 (d, $^3J_{H,H}$ = 6.6 Hz, 12 H; 2xCH(C*H*$_3)_2$), 0.33 (d, $^3J_{H,H}$ = 6.4 Hz, 24 H; 4xCH(C*H*$_3)_2$), -0.04 (d, $^3J_{H,H}$ = 6.8 Hz, 12 H; 2xCH(C*H*$_3)_2$) ppm. ^{13}C NMR (75.5 MHz, d_8-THF) δ 158.0 (C^{Ar}), 156.3 (C^{Ar}), 156.1 (C^{Ar}), 156.0 (C^{Ar}), 155.7 (C^{Ar}), 154.1 (C^{Ar}), 140.0 (C^{Ar}), 130.5 (C^{Ar}), 130.2 (C^{Ar}), 129.8 (C^{Ar}), 129.7 (C^{Ar}), 124.7 (C^{Ar}), 124.6 (C^{Ar}), 124.4 (C^{Ar}), 123.1 (C^{Ar}), 122.0 (C^{Ar}), 44.7 (*C*H$(CH_3)_2$), 44.5 (*C*H$(CH_3)_2$), 41.6 (CH(*C*H$_3)_2$), 40.6 (*C*H$(CH_3)_2$), 40.4 (*C*H$(CH_3)_2$), 37.5 (CH(*C*H$_3)_2$), 30.1 (CH(*C*H$_3)_2$), 28.9 (CH(*C*H$_3)_2$), 26.3 (CH(*C*H$_3)_2$), 25.7 (CH(*C*H$_3)_2$), 24.6

($CH(CH_3)_2$), 23.6 ($CH(CH_3)_2$) ppm. UV-vis (benzene) λ_{max} (ε, L $cm^{-1}mol^{-1}$) 850 (344), 658 (893), 580 (-), 490 (9882), 380 (-) nm. ATR-FTIR $\tilde{\upsilon}$ 3041 (w), 2952 (m), 1788 (m), 1565 (w), 1565 (w), 1458 (m), 1234 (m), 1010 (m), 881 (s), 795 (m), 727 (m), 615 (w), 534 (s), 390 (m) cm^{-1}. Raman (140 mW, 10 scans) 252 (19), 283 (16), 453 (20), 497 (19), 551 (19), 596 (31), 730 (10), 795 (9), 883 (8), 1044 (24), 1232 (57), 1342 (5328), 1675 (49), 1916 (2530) cm^{-1}.

Analytical data for *cyclo*-$(Dipp_2Sn)_3$ (**5**):

Yellow rods. m.p.^{exp} >239°C (decomp.). Anal. Calcd. for $C_{72}H_{102}Sn_3$ ($Dipp_6Sn_3$): C, 65.33; H, 7.77. Found: C, 65.04; H, 7.82. ^{1}H NMR (300.22 MHz, C_6D_6) δ 7.22-7.20 (m, 6 H; 6xH^{Ar}), 7.09-7.02 (m, 12 H; 12xH^{Ar}) 3.33-3.21 (m, 12 H; 12x$CH(CH_3)_2$), 1.41 (d, $^3J_{H,H}$ = 6.6 Hz, 18 H; 3x$CH(CH_3)_2$), 1.16 (d, $^3J_{H,H}$ = 6.5 Hz, 18 H; 3x$CH(CH_3)_2$), 0.78 (d, $^3J_{H,H}$ = 6.5 Hz, 18 H; 3x$CH(CH_3)_2$), 0.52 (d, $^3J_{H,H}$ = 6.4 Hz, 18 H; 3x$CH(CH_3)_2$) ppm. ^{13}C NMR (75.5 MHz, C_6D_6) δ 154.9 (C^{Ar}), 154.8 (C^{Ar}), 146.4 (C^{Ar}), 129.5 (C^{Ar}), 124.7 (C^{Ar}), 124.0 (C^{Ar}), 40.5 ($CH(CH_3)_2$), 39.2 ($CH(CH_3)_2$), 27.2 ($CH(CH_3)_2$), 26.9 ($CH(CH_3)_2$), 26.0 ($CH(CH_3)_2$), 25.3 ($CH(CH_3)_2$) ppm. ^{119}Sn NMR (111.92 MHz, C_6D_6) δ -365.8 ($^1J_{Sn,117Sn}$ = 3113 Hz) ppm.

Synthesis of $Bi_8Sn_3Dipp_6$ (4)

A solution of 460 mg $Bi[N(SiMe_3)_2]_3$ (0.67 mmol, 2.0 eq) in 4 mL DME was added dropwise to 443 mg $Dipp_2SnH_2$ (1.0 mmol, 3.0 eq) also dissolved in 4 mL DME. The solution turned briefly red and then the color slowly faded to reddish brown. After 2 days $Bi_4Sn_4H_2Dipp_6$ (**6**) crystallized from the dark brownish red solution as red-brown rhombic plates. The supernatant solution was concentrated to one third by volume via slow evaporation of the solvent to give an oily solid. The oily solid was extracted in 5 mL *n*-pentane, filtered and stored at -30°C to give the product as brownish red rods suitable for single crystal X-ray diffraction after 2 days. The remaining material after extraction with *n*-pentane was redissolved in DME to yield an orange brown solution from which after storage at -30°C yellow crystals of **5** together with a very small amount of **7** were obtained.

Analytical data for $Bi_8Sn_3Dipp_6$ (**4**):

Yield: 150 mg (15% yield referred to $Dipp_2SnH_2$, 60% yield referred to $Bi[N(SiMe_3)_2]_3$), brownish red needles. m.p.^{exp} >188°C (decomp.). Anal. Calcd. for $C_{80}H_{122}Bi_8O_4Sn_3$ ($Bi_8Sn_3Dipp_6$*2 DME): C, 30.26; H, 3.87. Found: C, 30.01; H, 3.95. ^{1}H NMR (300.22 MHz, d_8-THF, -40°C) δ 7.19-7.17 (m, 12 H; 12x*m*-H^{Ar}), 6.90-6.87 (m, 6 H; 6x*p*-H^{Ar}), 3.81 (sept, $^3J_{H,H}$ = 6.5 Hz, 6 H; 3x$CH(CH_3)_2$), 2.64 (sept, $^3J_{H,H}$ = 6.5 Hz, 6 H; 3x$CH(CH_3)_2$), 1.70 (d, $^3J_{H,H}$ = 6.5 Hz, 18 H; 3x$CH(CH_3)_2$, overlay with solvent peak), 1.32 (d, $^3J_{H,H}$ = 6.5 Hz, 18 H; 3x$CH(CH_3)_2$), 1.10 (d, $^3J_{H,H}$ = 6.5 Hz, 18 H; 3x$CH(CH_3)_2$), 0.13 (d, $^3J_{H,H}$ = 6.5 Hz, 18 H; 3x$CH(CH_3)_2$) ppm. ^{13}C NMR (75.5 MHz, d_8-THF, -20°C) δ 155.5 (C^{Ar}), 154.2 (C^{Ar}), 153.6 (C^{Ar}), 129.6 (C^{Ar}), 126.4 (C^{Ar}), 126.0 (C^{Ar}), 40.7 ($CH(CH_3)_2$), 36.9 ($CH(CH_3)_2$), 34.0 ($CH(CH_3)_2$), 28.0 ($CH(CH_3)_2$), 27.0 ($CH(CH_3)_2$), 22.5 ($CH(CH_3)_2$) ppm. ^{119}Sn NMR (111.92 MHz, d_8-THF) δ -946.2 (broad, $Tripp_2$*Sn*) ppm. ^{119}Sn NMR (111.92 MHz, C_6D_6) δ -940.5 (broad, $Tripp_2$*Sn*) ppm. UV-Vis (THF) λ_{max} (ε, L $cm^{-1}mol^{-1}$) 654 (1512), 574 (4635), 485 (7912), 441 (9553), 376 (-), 306 (-) nm. Raman (140 mW, 10 scans) 247 (55), 392 (47), 449 (48), 502 (48), 552 (49), 596 (57), 732 (48), 798 (46), 880 (48), 1046 (60), 1103 (59), 1233 (83), 1341 (100) cm^{-1}.

Analytical data of *cyclo*-$(Dipp_2Sn)_3$ (**5**) is identical to **5** isolated from the synthesis of $Bi_4Sn_4H_2Dipp_6$ (**6**).

3 NMR spectroscopy

General

^{1}H (300.22 MHz), ^{13}C (75.5 MHz), as well as ^{119}Sn (111.92 MHz), NMR spectra were recorded on a Varian Mercury 300 MHz spectrometer from Varian at 25°C if not otherwise stated. Spectra were referenced to residual solvent signals or with an external reference. Chemical shifts are given in ppm relative to TMS regarding ^{1}H, ^{13}C, ^{29}Si. ^{119}Sn resonances are given relative to Me_4Sn. Coupling constants (^{n}J) are reported in Hertz (Hz). Deuterated solvents applied in NMR experiments were degassed using the *freeze-pump method* and dried over activated 3 Å molecular sieves without any further purification.

NMR spectra

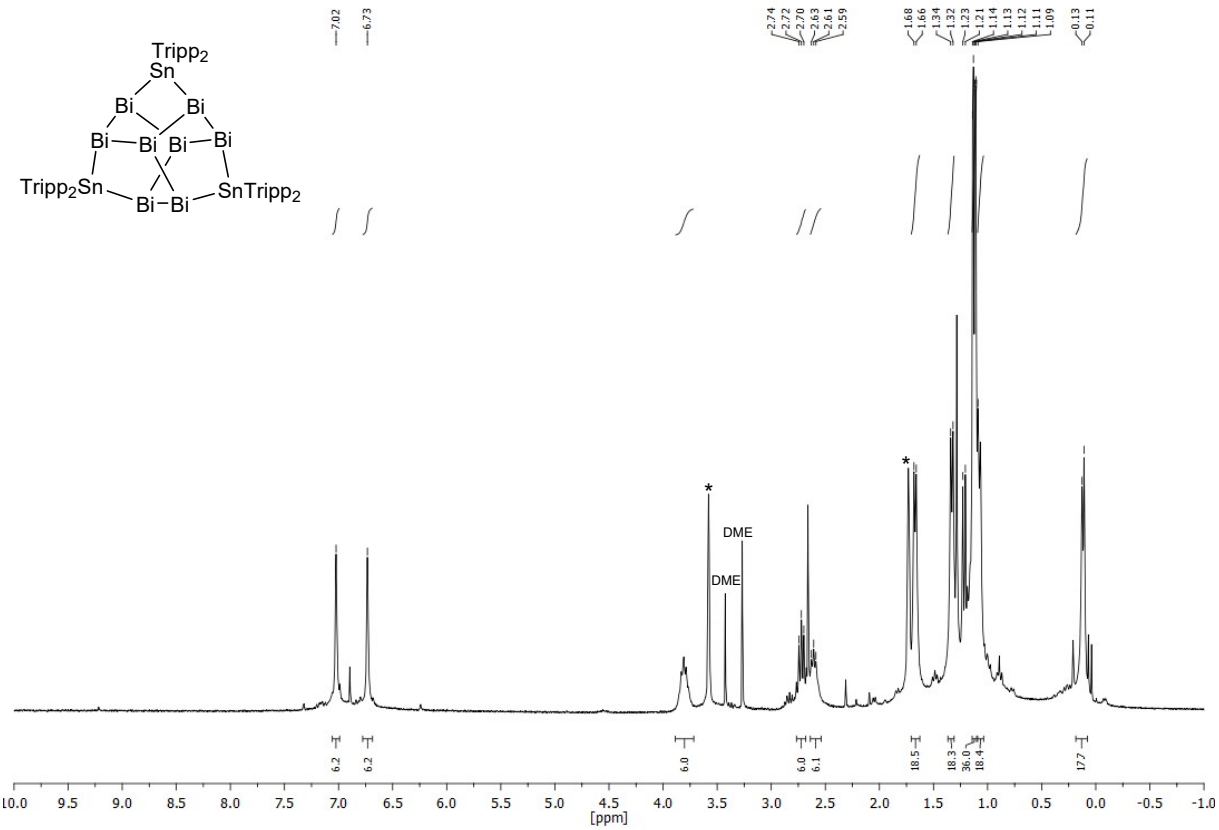

Figure S 1 ^{1}H NMR spectrum of $Bi_8Sn_3Tripp_6$ (**1**) at -10°C in d_8-THF (* marks residual solvent peaks).

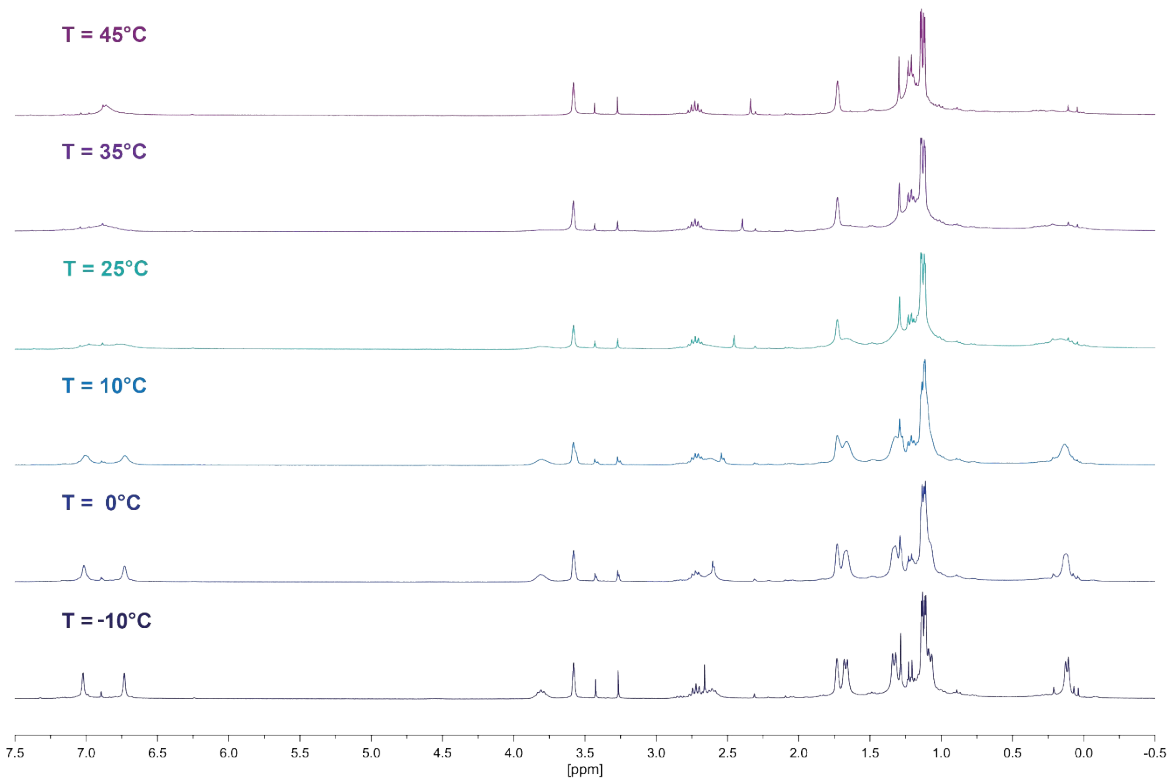

Figure S 2 VT-^{1}H NMR of $Bi_8Sn_3Tripp_6$ (**1**) in d_8-THF at 45, 35, 25, 10, 0 and -10°C, respectively (top to bottom).

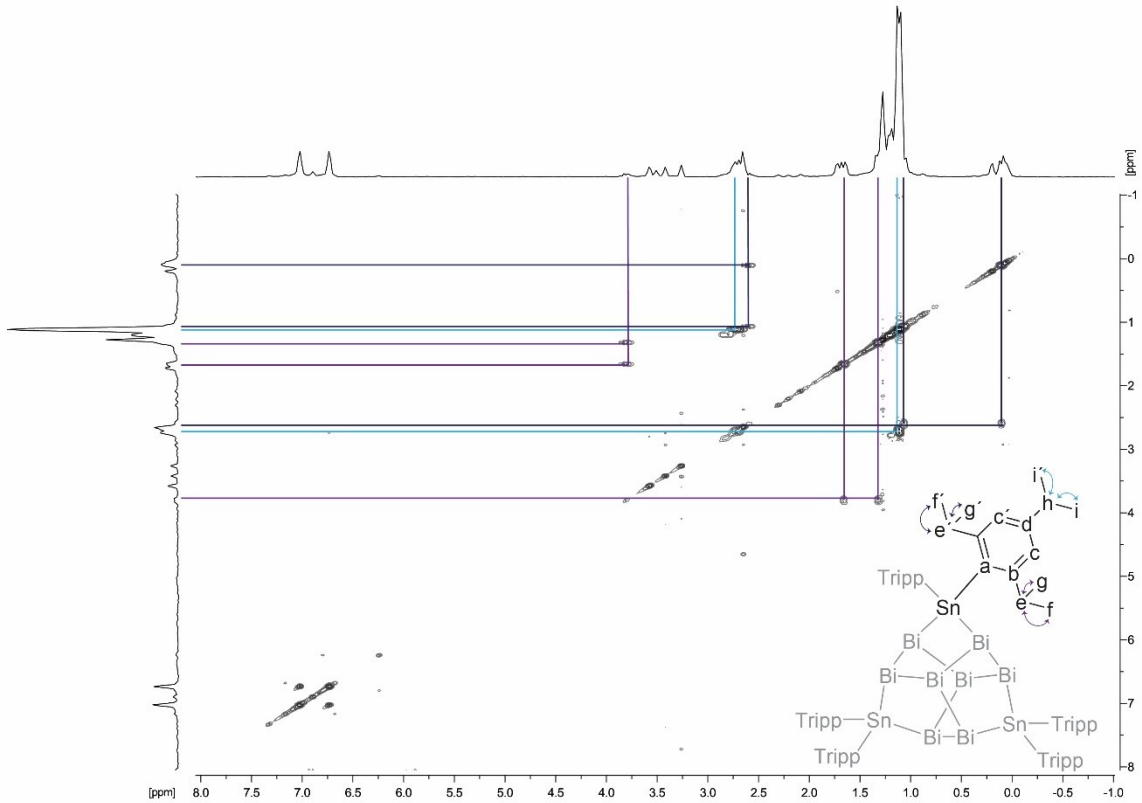

Figure S 3 2D-^{1}H,^{1}H-COSY spectrum of $Bi_8Sn_3Tripp_6$ (**1**) at -10°C d_8-THF.

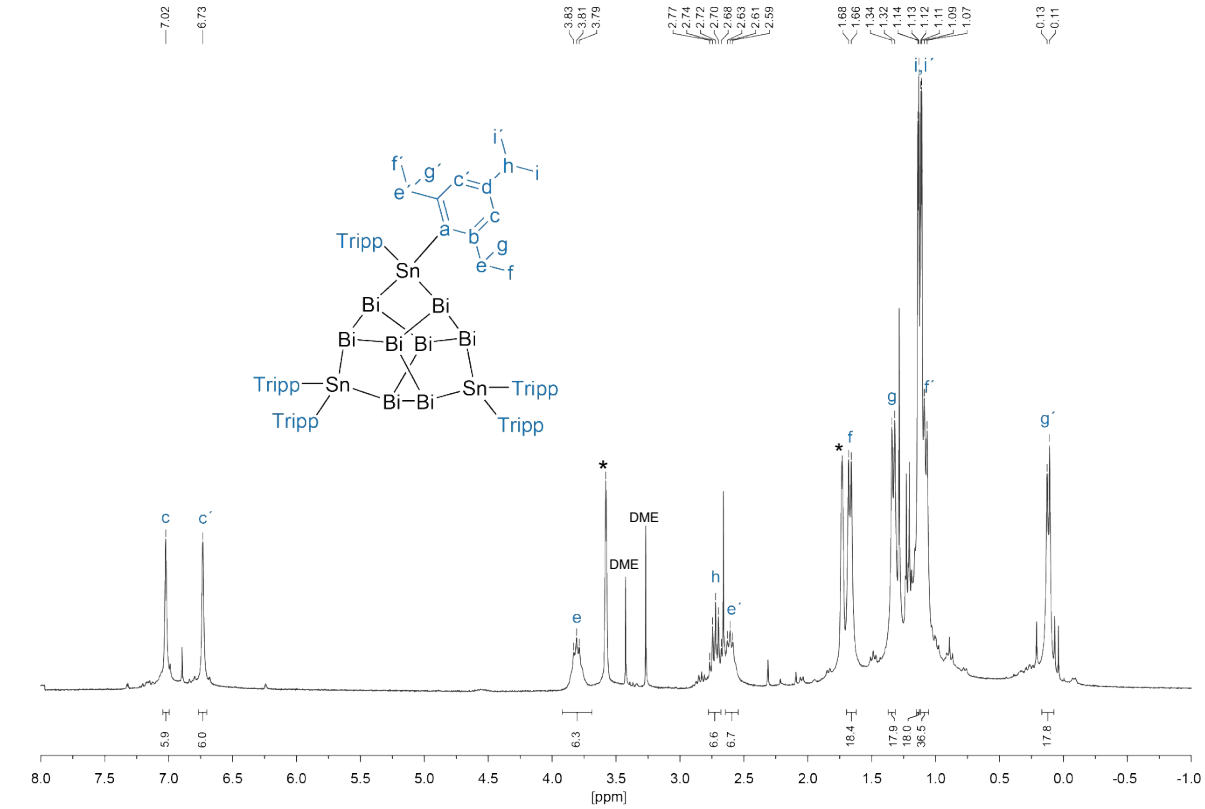

Figure S 4 Assigned ^{1}H NMR spectrum of $Bi_8Sn_3Tripp_6$ (**1**) at -10°C in d_8-THF (* marks residual solvent peaks).

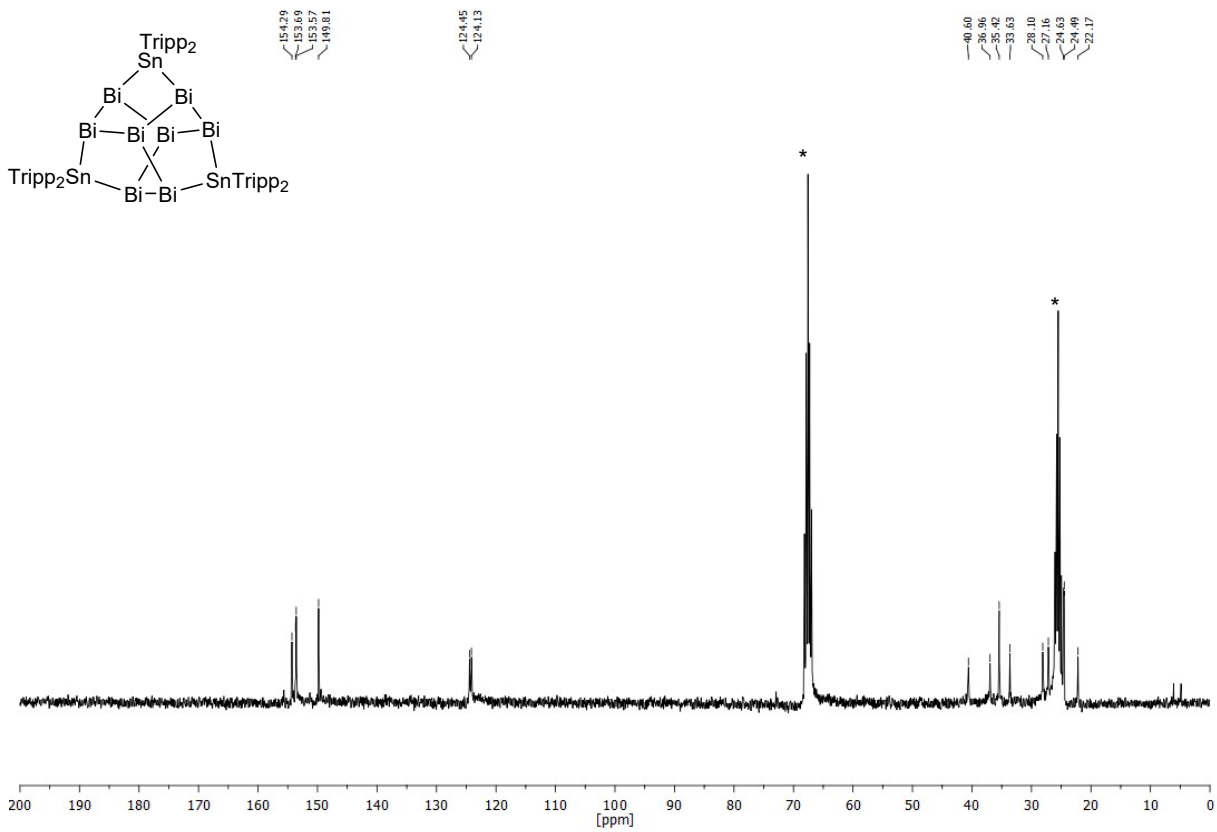

Figure S 5 ^{13}C NMR spectrum of $Bi_8Sn_3Tripp_6$ (**1**) at -10°C in d_8-THF (* marks residual solvent peaks).

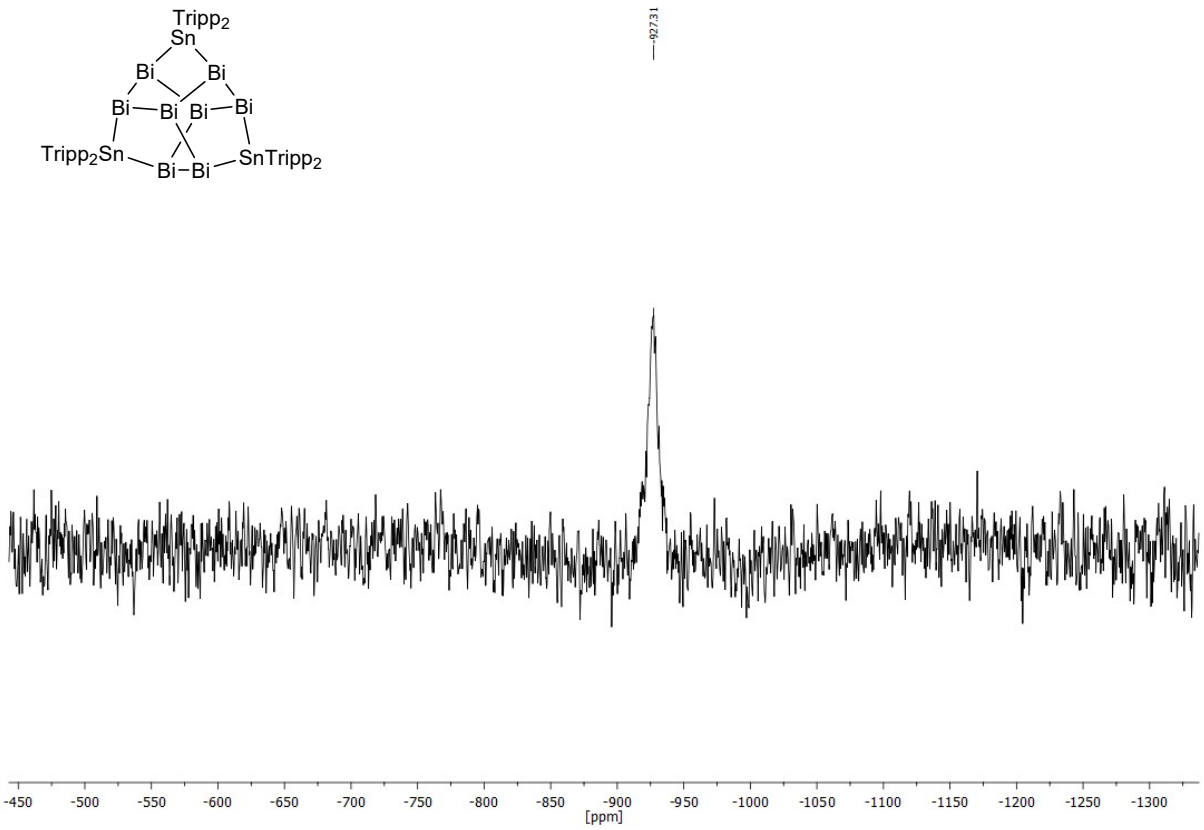

Figure S 6 $^{119}Sn\{^{1}H\}$ NMR spectrum of $Bi_8Sn_3Tripp_6$ (**1**) at rt in d_8-THF.

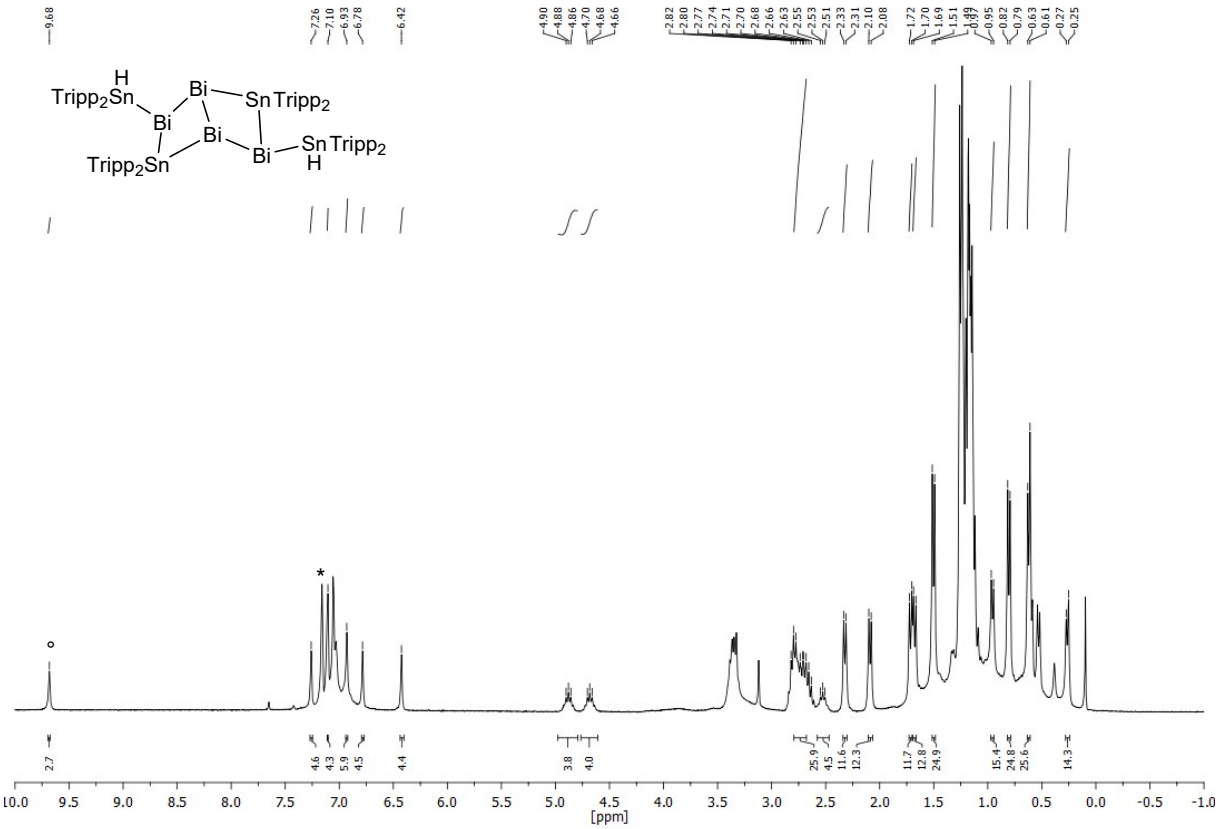

Figure S 7 ^{1}H NMR spectrum of $Bi_4Sn_4H_2Tripp_8$ (**3**) in C_6D_6 (* marks residual solvent peaks). The Sn*H* signal is marked with °. No coupling satellites ($^{1}J_{1H,117/119Sn}$) are observed.

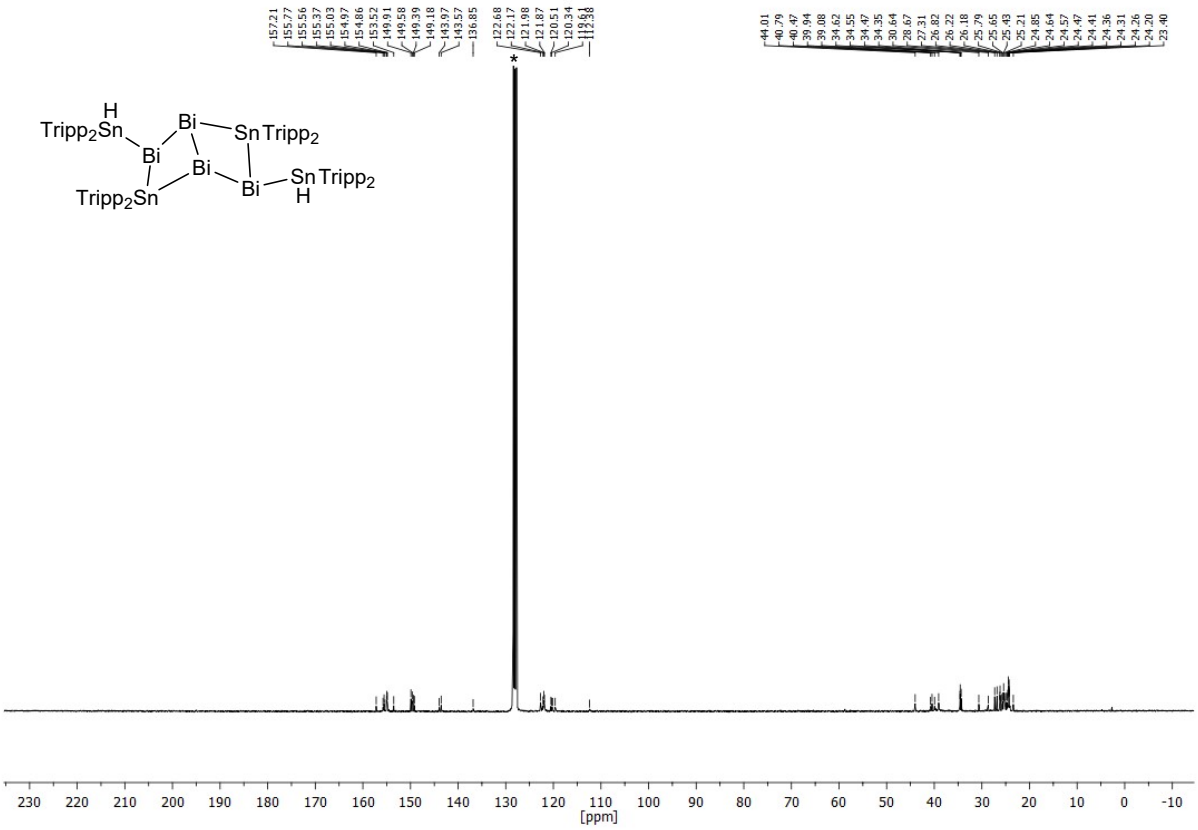

Figure S 8 ^{13}C NMR spectrum of $Bi_4Sn_4H_2Tripp_8$ (**3**) in C_6D_6 (* marks residual solvent peaks).

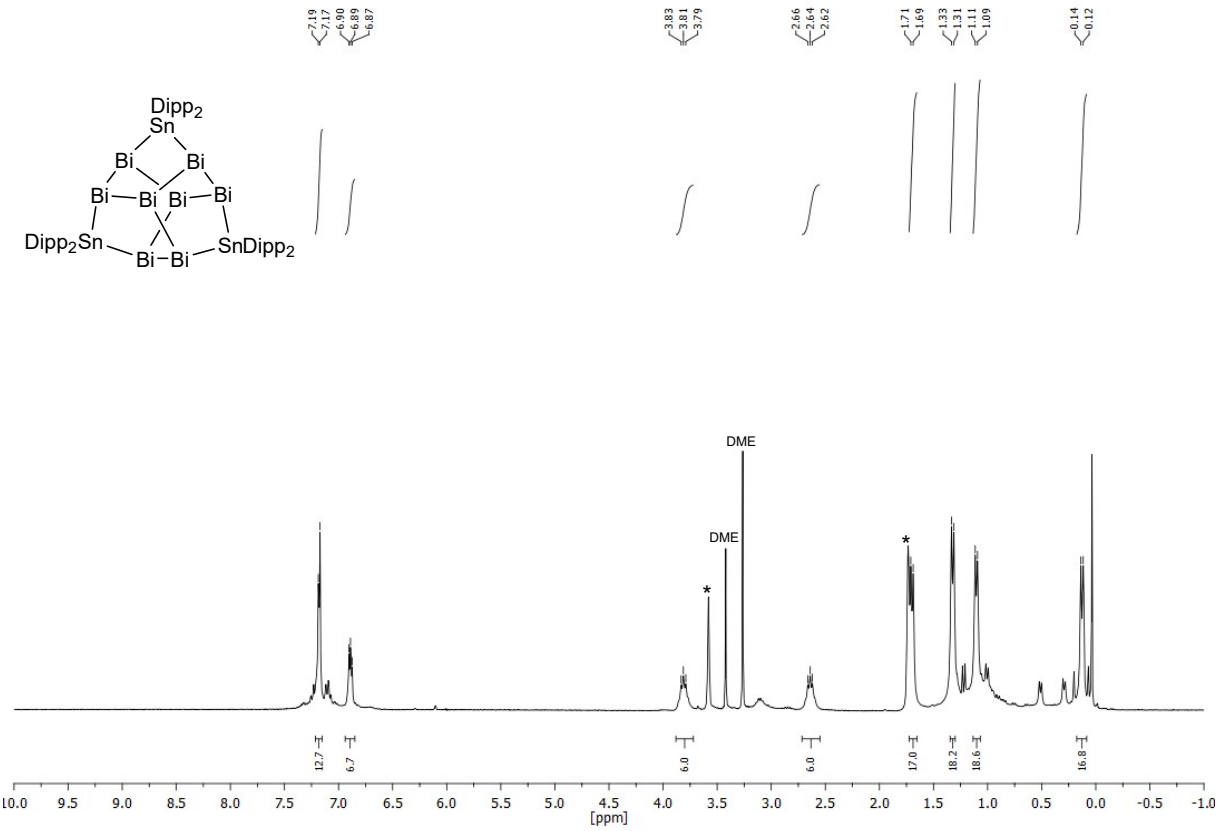

Figure S 9 ^{1}H NMR spectrum of $Bi_8Sn_3Dipp_6$ (**4**) at -40°C in d_8-THF (* marks residual solvent peaks).

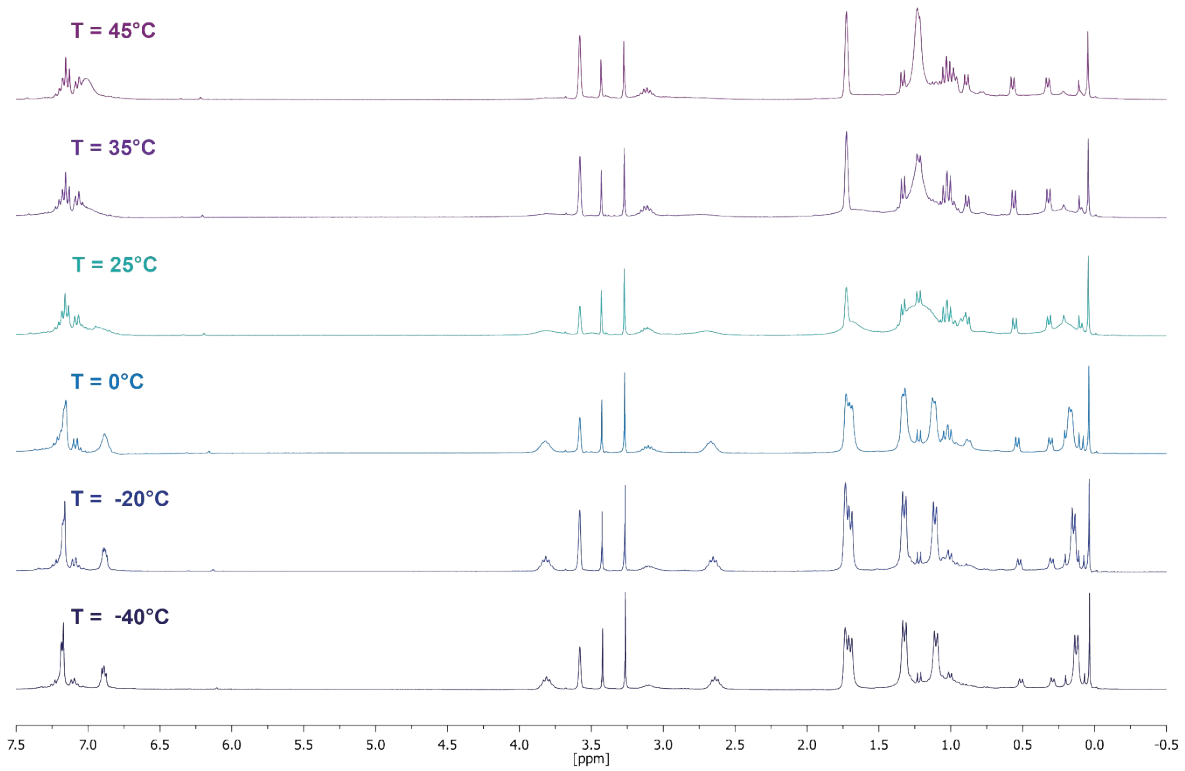

Figure S 10 VT-^{1}H NMR of $Bi_8Sn_3Dipp_6$ (**4**) in d_8-THF at 45, 35, 25, 10, 0 and -10°C, respectively (top to bottom).

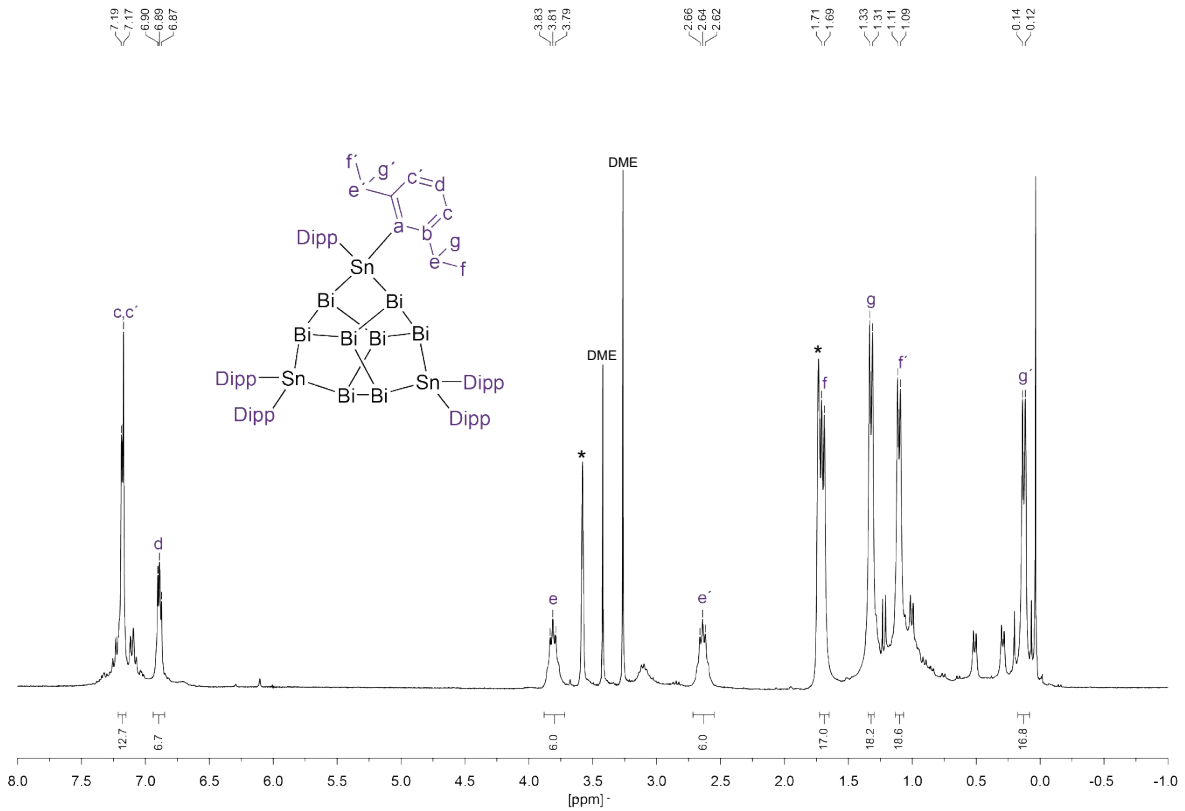

Figure S 11 Assigned ^{1}H NMR spectrum of $Bi_8Sn_3Dipp_6$ (**4**) at -10°C in d_8-THF (* marks residual solvent peaks).

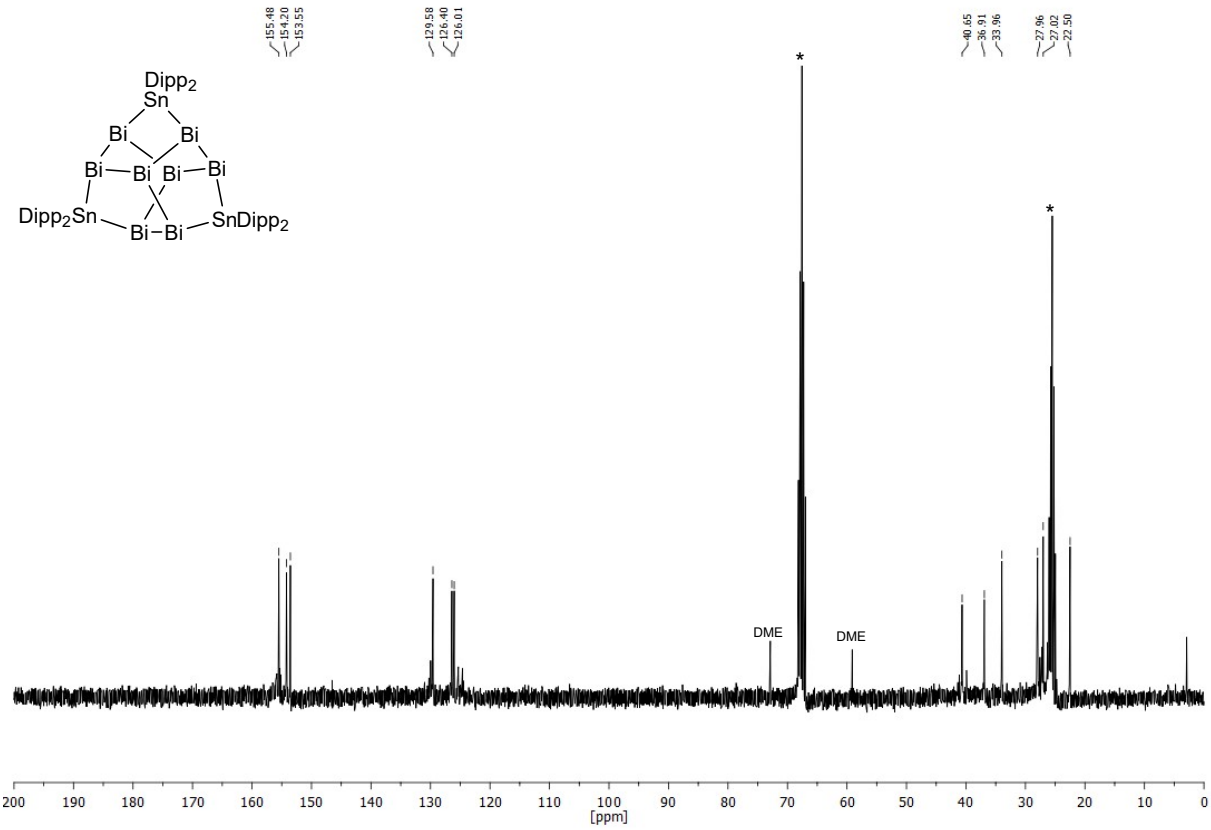

Figure S 12 ^{13}C NMR spectrum of $Bi_8Sn_3Dipp_6$ (**4**) at -40°C in d_8-THF (* marks residual solvent peaks).

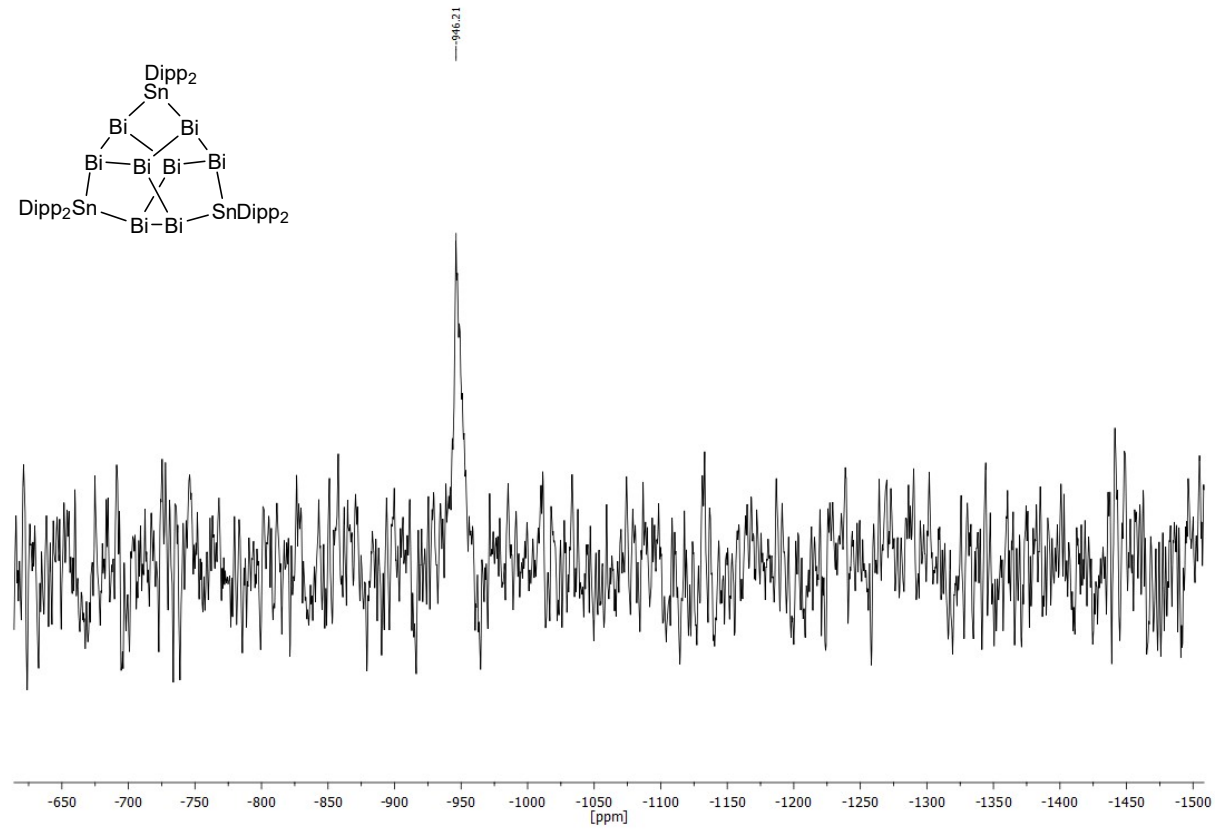

Figure S 13 ^{119}Sn{^{1}H} NMR spectrum of $Bi_8Sn_3Dipp_6$ (**4**) at rt in d_8-THF.

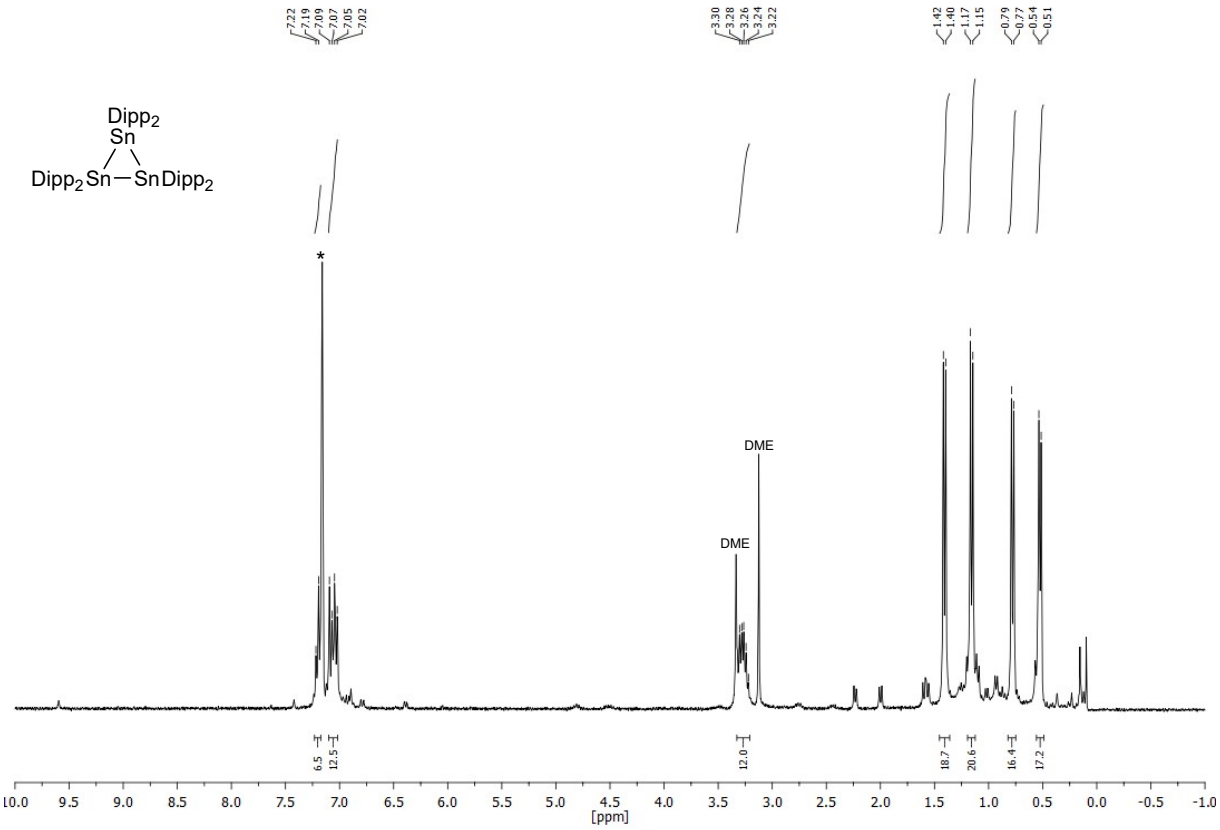

Figure S 14 ^{1}H NMR spectrum of *cyclo*-$(Dipp_2Sn)_3$ (**5**) in C_6D_6 (* marks residual solvent peaks).

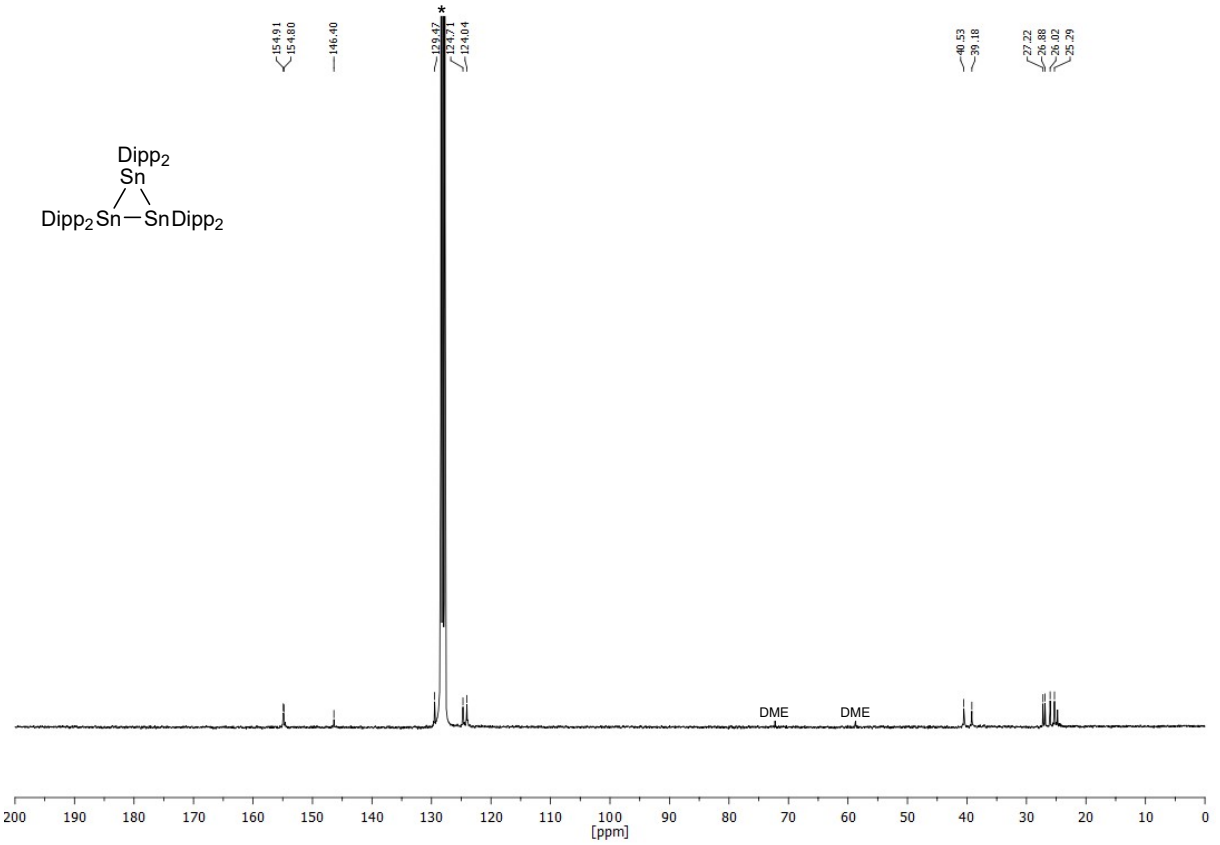

Figure S 15 ^{13}C NMR spectrum of *cyclo*-$(Dipp_2Sn)_3$ (**5**) in C_6D_6 (* marks residual solvent peaks).

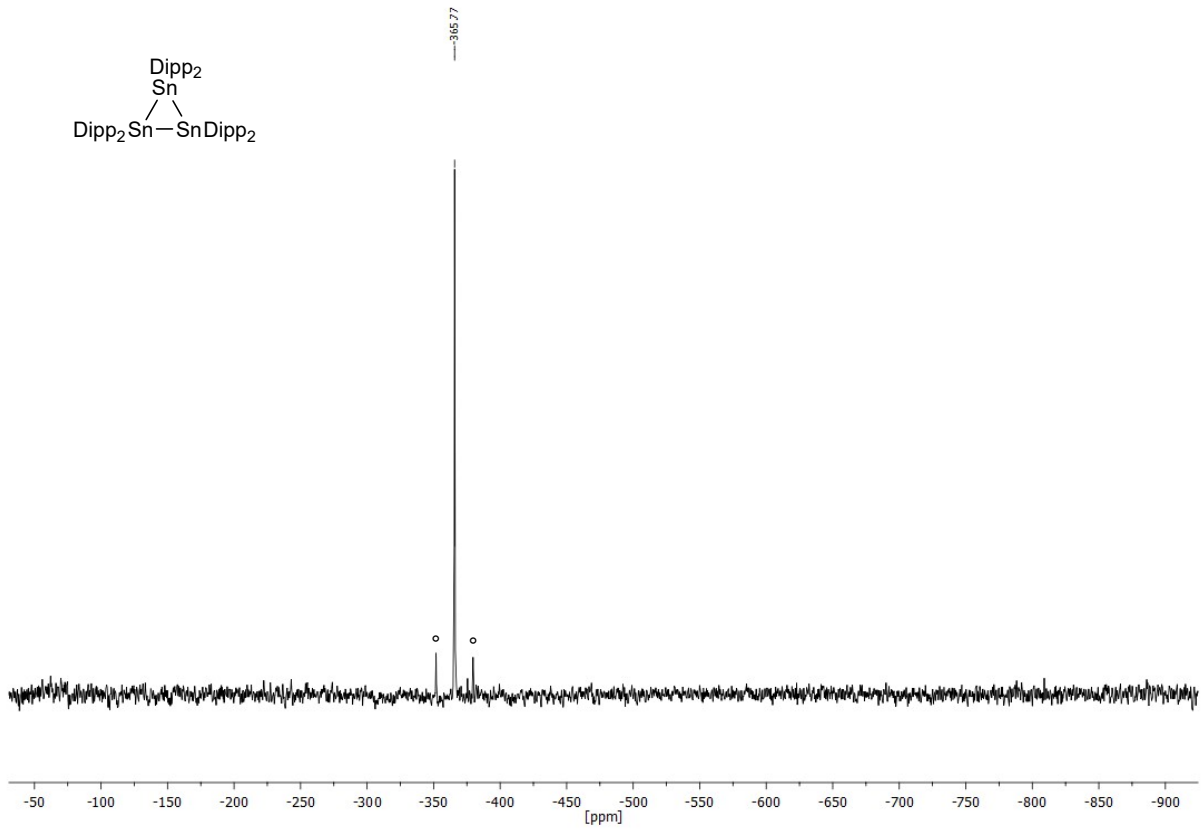

Figure S 16 ^{119}Sn{^{1}H] NMR spectrum of *cyclo*-(Dipp$_2$Sn)$_3$ (**5**) in C_6D_6. The ° indicates coupling satellites: $^{1}J_{119Sn,117Sn}$= 3113 Hz.

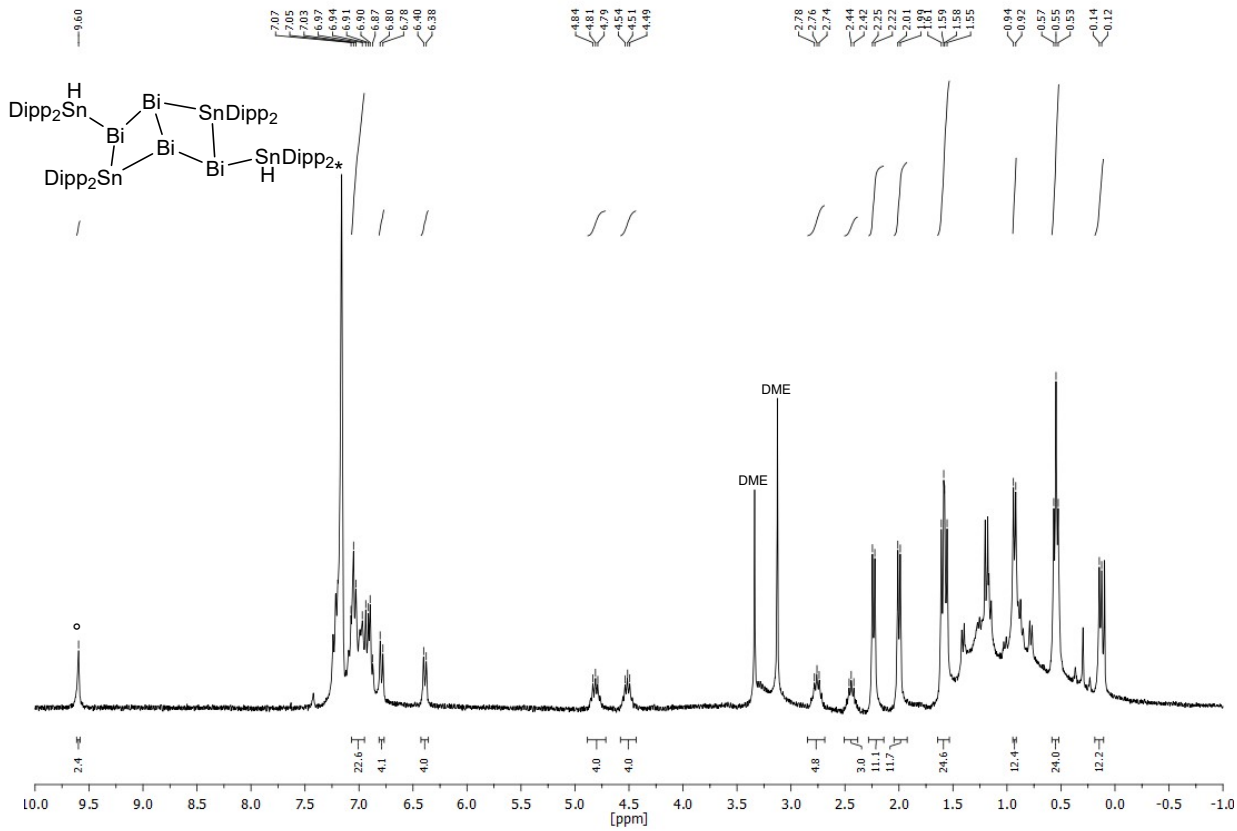

Figure S 17 ^{1}H NMR spectrum of $Bi_4Sn_4H_2Dipp_8$ (**6**) in C_6D_6 (* marks residual solvent peak). The Sn*H* signal is marked with °. No coupling satellites ($^{1}J_{1H,117/119Sn}$) are observed.

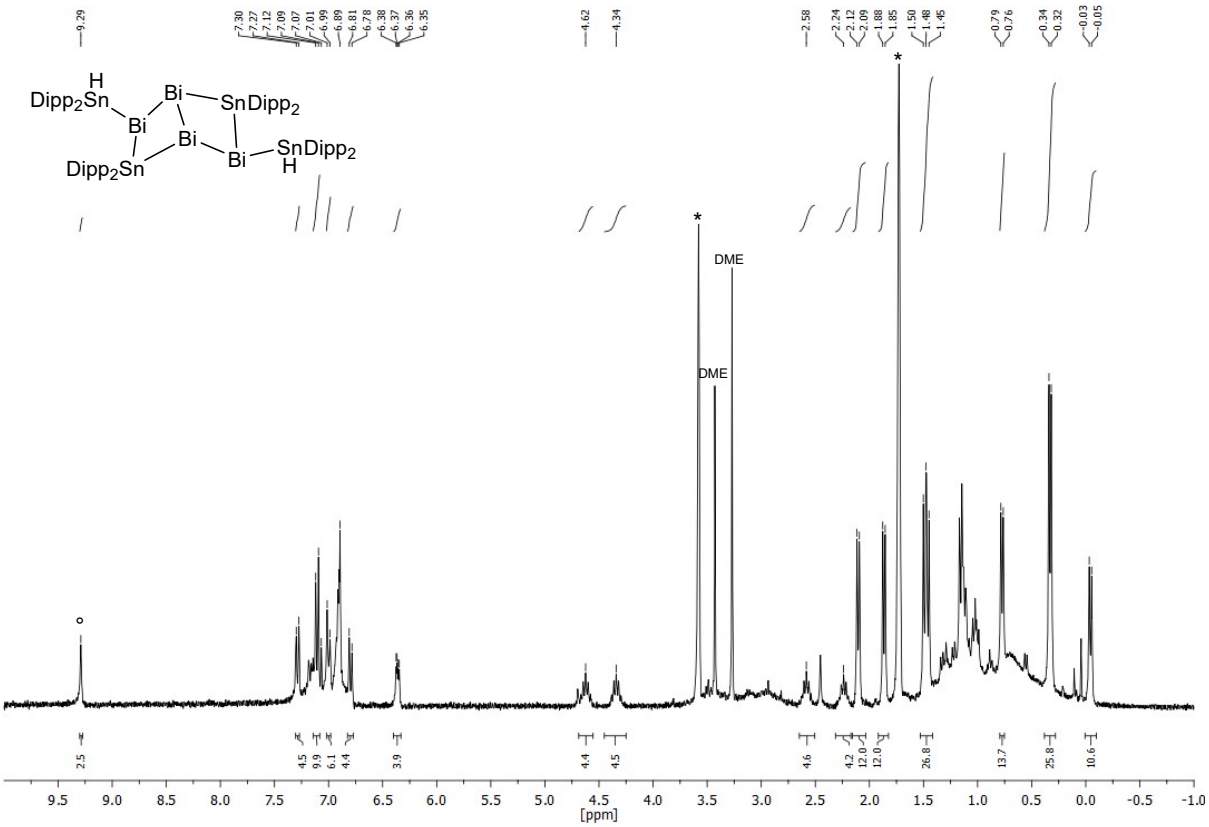

Figure S 18 ^{1}H NMR spectrum of $Bi_4Sn_4H_2Dipp_8$ (**6**) in d_8-THF (* marks residual solvent peaks). The Sn*H* signal is marked with °. No coupling satellites ($^{1}J_{1H,117/119Sn}$) are observed.

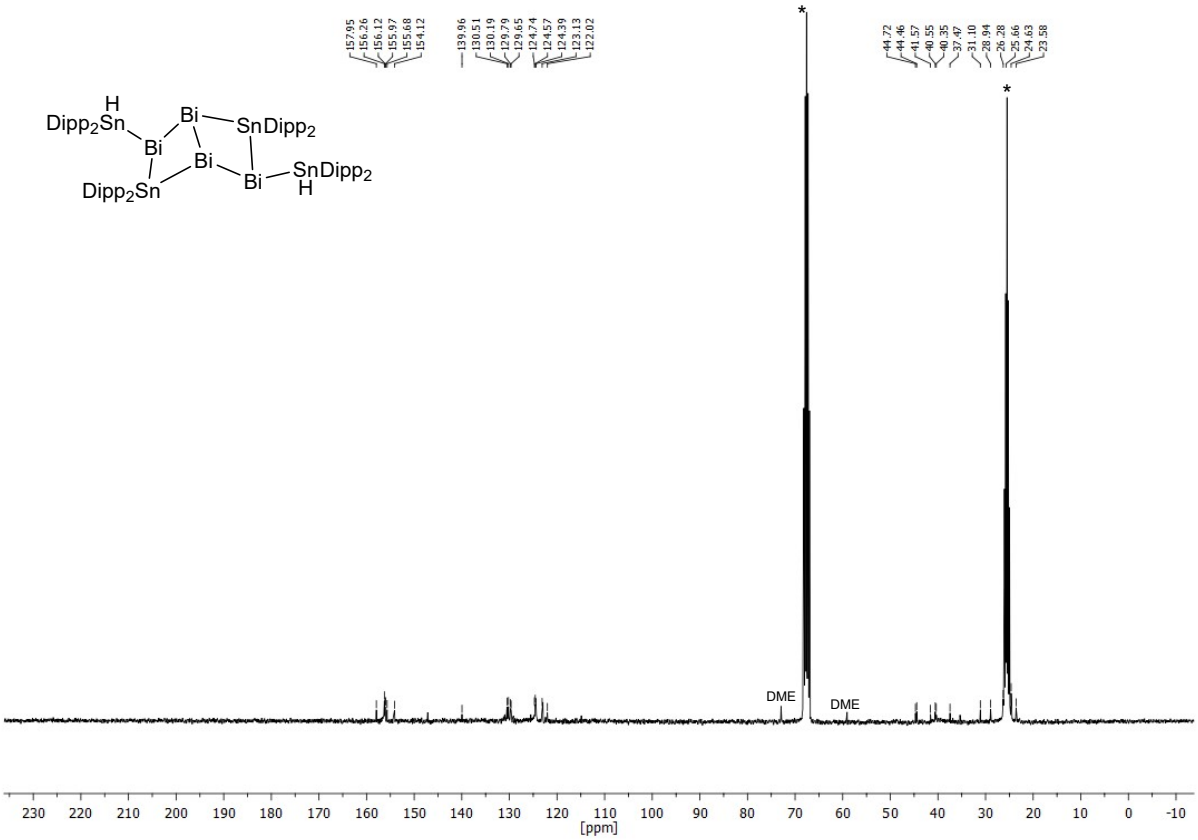

Figure S 19 ^{13}C NMR spectrum of $Bi_4Sn_4H_2Dipp_8$ (**6**) in d_8-THF (* marks residual solvent peaks).

4 UV-Vis spectroscopy

General

All UV-Vis measurements were performed in quartz glass cuvettes with a thickness of 1 cm on a Cary 60 UV-Vis device from Agilent Technologies. All measurements were done in absorption mode. Absorption maxima are given in nm. Extinction coefficents (ε) are given in L $cm^{-1}mol^{-1}$. (see 2 Experimental Details)

UV-Vis spectra

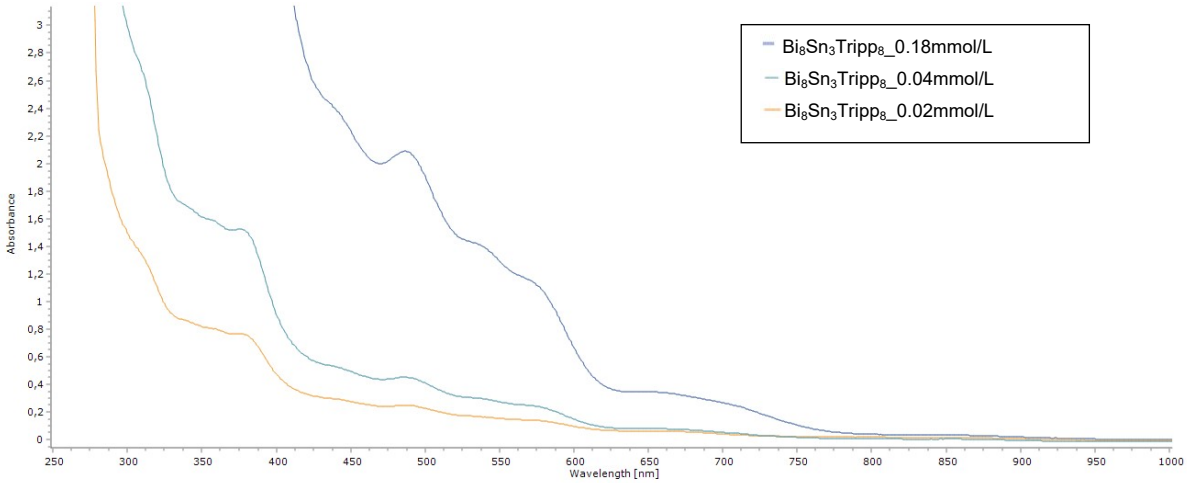

Figure S 20 UV-Vis spectra of $Bi_8Sn_3Tripp_6$ (**1**).

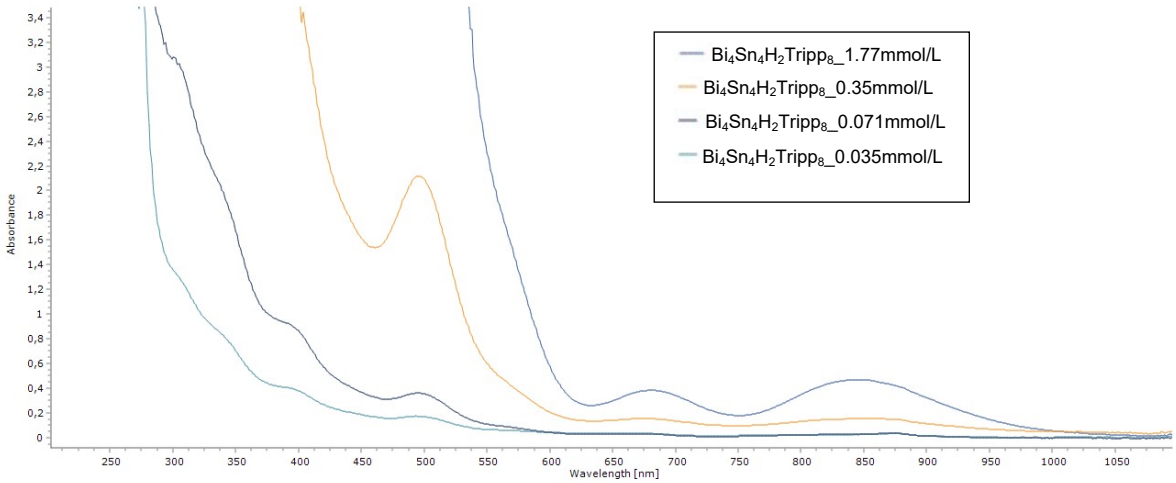

Figure S 21 UV-Vis spectra of $Bi_4Sn_4H_2Tripp_8$ (**3**).

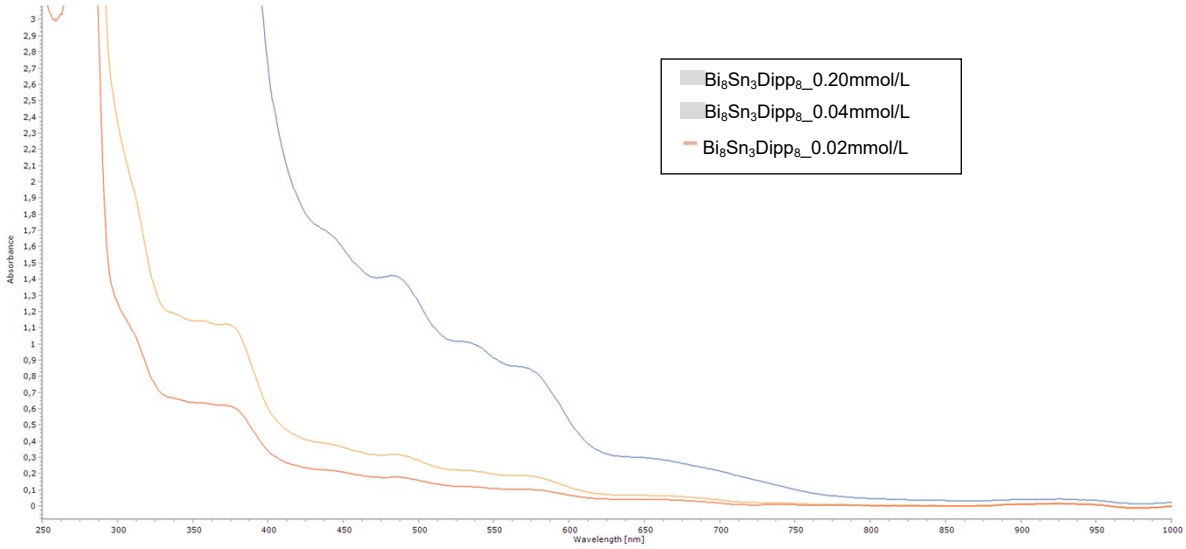

Figure S 22 UV-Vis spectra of $Bi_8Sn_3Dipp_6$ (**4**).

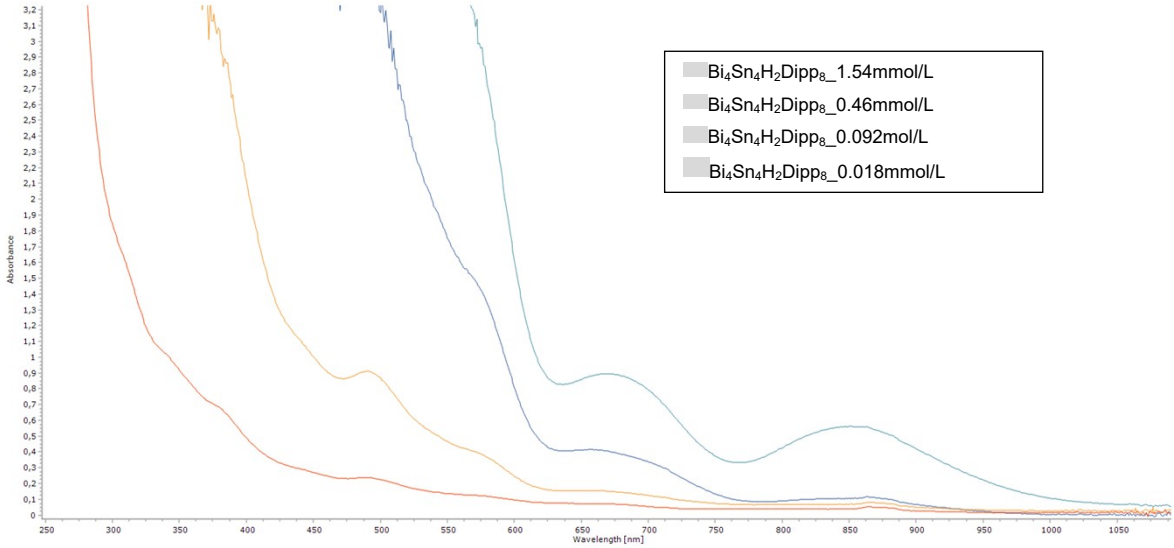

Figure S 23 UV-Vis spectra of $Bi_4Sn_4H_2Dipp_8$ (**6**).

5 ATR-FTIR and Raman spectroscopy

General

All IR measurements were measured fast under ambient conditions on an ALPHA-P device from Bruker in transmission modus. The letters s (strong), m (medium) and w (weak) are used to indicate the intensity of the transmission bands (see 2 Experimental Details). All Raman measurements were performed in a capillary using a Perkin Elmer Raman Station 400F with a build-in 350 mW laser operating at 785 nm.

ATR-FTIR and Raman spectra

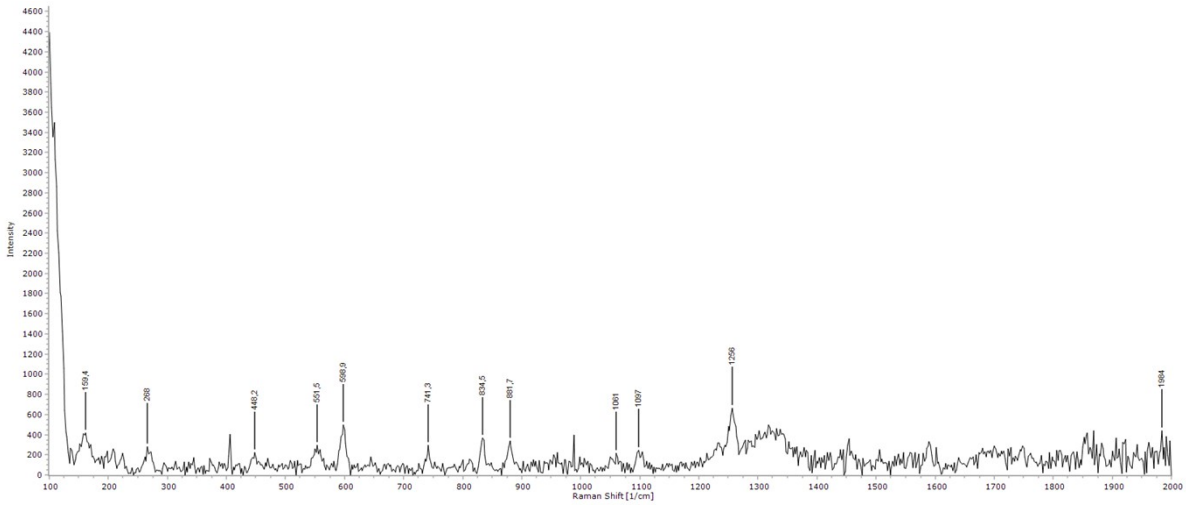

Figure S 24 Raman spectrum of $Bi_8Sn_3Tripp_6$ (**1**).

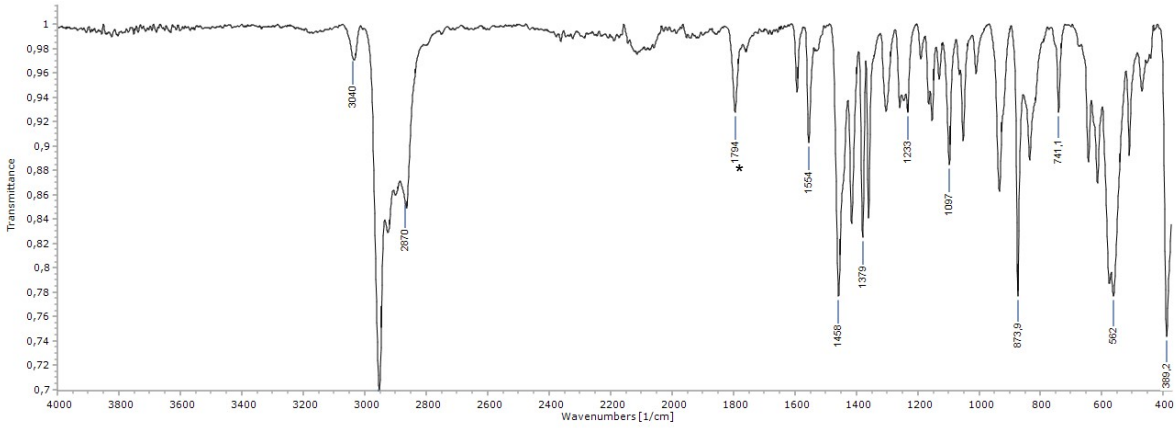

Figure S 25 ATR-FTIR spectrum of $Bi_4Sn_4H_2Tripp_8$ (**3**). The * indicates the SnH vibration at 1794 cm^{-1}.

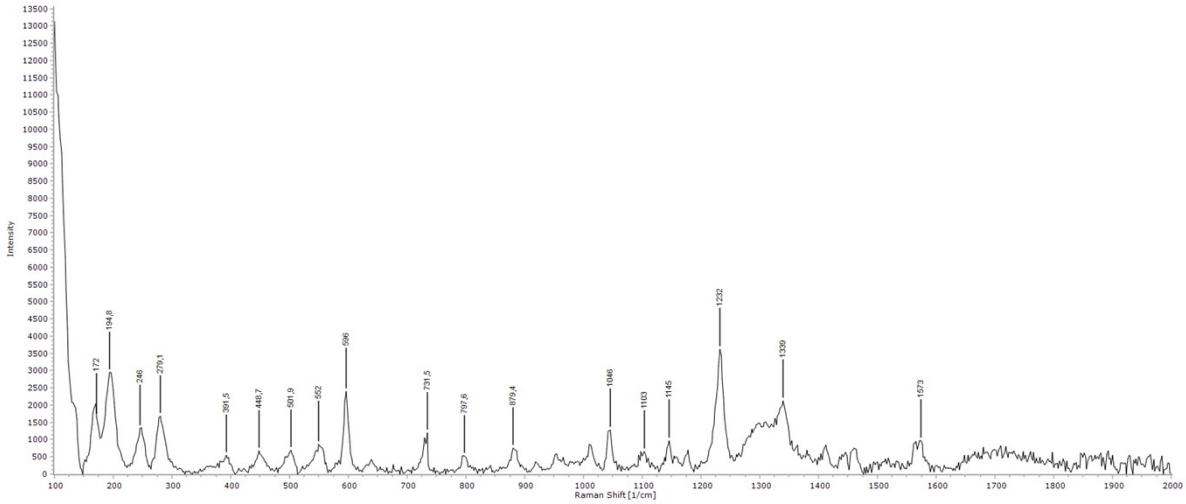

Figure S 26 Raman spectrum of $Bi_8Sn_3Dipp_6$ (**4**).

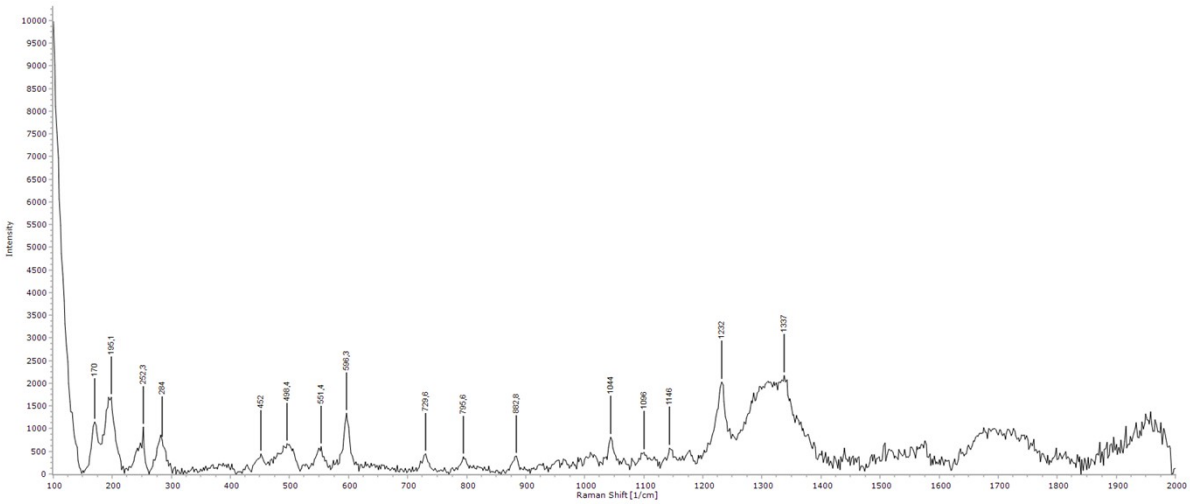

Figure S 27 Raman spectrum of $Bi_4Sn_4H_2Dipp_8$ (**6**).

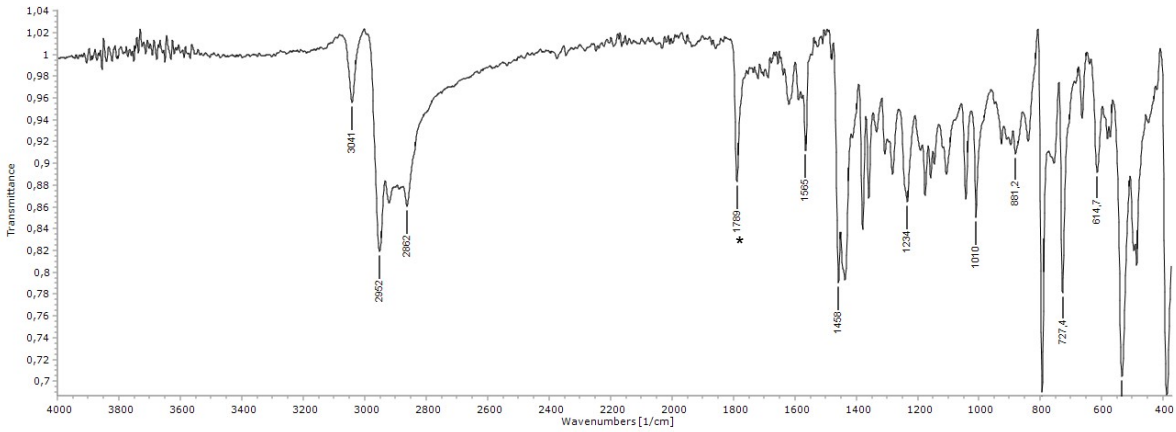

Figure S 28 ATR-FTIR spectrum of $Bi_4Sn_4H_2Dipp_8$ (**6**). The * indicates the SnH vibration at 1788 cm^{-1}.

6 Details of XRD measurements, structure solution and refinement

General

For single crystal X-ray diffractometry all suitable crystals were covered with a layer of silicone oil. A single crystal was selected, mounted on a glass rod on a copper pin, and placed in the cold N_2 stream provided by an Oxford Cryosystems cryometer (T = 100 K), if not otherwise stated. XRD data collection was performed on a Bruker APEX II diffractometer with use of Mo Kα radiation (λ = 0.71073 Å) from an IμS microsource and a CCD area detector. Empirical absorption corrections were applied using SADABS[4,5]. The structures were solved with use of either direct methods or the Patterson option in SHELXS. Structure refinement was carried out using SHELXL[6,7]. CIF files were edited, validated and formatted with the program OLEX2[8]. The space group assignments and structural solutions were evaluated using PLATON.[9,10] All non-hydrogen atoms were refined anisotropically. Hydrogen atoms next to the heavy atom Sn were located on the difference Fourier map in solid state structures of $Bi_4Sn_4H_2Dipp_8$ (**6**). However, we were not able to locate hydrogens connected to Sn atoms in the Fourier difference map in $Bi_4Sn_4H_2Tripp_8$ (**3**). Instead, hydrogen atoms were placed using a riding model for these structures. All other hydrogen atoms were placed in calculated positions corresponding to standard bond lengths and angles also using riding models. Table S 2 to Table S 4 contain crystallographic data and details for measurements and refinement. Bond lengths of Bi-Bi bonds in cluster compounds exceed standard single Bi-Bi bond lengths and hence are not recognized as bonding in checkcif reports. Residue electron densities at heavy atoms are ascribed to fourier truncation and absorption effects. CCDC numbers 2072047 to 2072052 contain the supplementary crystallographic data for compound in this paper. These data can be obtained free of charge via www.ccdc.cam.ac.uk/data_request/cif.

Table S 2 Crystal data and structure refinement of compounds **1** and **6**.

Compound	$Bi_8Sn_3Tripp_6$ (**1**)	$Bi_4Sn_4H_2Dipp_8$ (**6**)
CCDC number	1072047	1072048
Empirical formula	$C_{96}H_{153}O_3Sn_3Bi_8$	$C_{100}H_{148}Bi_4O_2Sn_4$
Formula weight [g mol^{-1}]	3383.08	2692.86
Temperature [K]	99.92	100.11
Crystal system	Triclinic	triclinic
Space group	P-1	P-1
a [Å]	12.4251(8)	15.2666(9)
b [Å]	18.3927(12)	16.4529(8)
c [Å]	25.1535(18)	21.8940(12)
a [°]	103.471(3)	78.431(2)
β [°]	90.449(4)	80.056(2)
γ [°]	103.813(4)	75.059(2)
Volume [Å^3]	5416.3(6)	5162.8(5)
Z	2	2
ρ_{calc} [g cm^{-3}]	2.074	1.732
μ [mm^{-1}]	13.664	7.784
F(000)	3134.0	2592.0
Crystal size [mm^3]	0.22 × 0.15 × 0.11	0.29 × 0.25 × 0.12
Radiation	MoKα (λ = 0.71073)	MoKα (λ = 0.71073)
2Θ range for data collection [°]	3.61 to 52	3.17 to 52
Index ranges	-15 ≤ h ≤ 15, -22 ≤ k ≤ 22, -31 ≤ l ≤ 31	-18 ≤ h ≤ 18, -20 ≤ k ≤ 20, -27 ≤ l ≤ 26
Reflections collected	105823	145026
Independent reflections	21252 [R_{int} = 0.1357, R_{sigma} = 0.1011]	20225 [R_{int} = 0.1138, R_{sigma} = 0.0808]
Data/restraints/parameters	21252/666/1030	20225/13/1031
Goodness-of-fit on F^2	0.908	1.048
Final R indexes [I>=2σ (I)]	R_1 = 0.0430, wR_2 = 0.0919	R_1 = 0.0455, wR_2 = 0.0859
Final R indexes [all data]	R_1 = 0.0700, wR_2 = 0.1032	R_1 = 0.0718, wR_2 = 0.0965
Largest diff. peak/hole [e Å^{-3}]	2.33/-2.20	2.89/-2.60

Table S 3 Crystal data and structure refinement of compounds **5** and **4**.

Compound	*cyclo*-$(Dipp_2Sn)_3$ (**5**)	$Bi_8Sn_3Dipp_6$ (**4**)
CCDC number	1072050	1072049
Empirical formula	$C_{72}H_{102}Sn_3$	$C_{80}H_{122}Bi_8O_4Sn_3$
Formula weight [g mol^{-1}]	1323.60	3175.68
Temperature [K]	249.95	100.14
Crystal system	monoclinic	monoclinic
Space group	C2/c	C2/c
a [Å]	11.8602(7)	25.7205(9)
b [Å]	25.223(2)	16.5280(6)
c [Å]	22.4048(17)	23.0120(9)
a [°]	90	90
β [°]	94.905(3)	111.630(2)
γ [°]	90	90
Volume [Å^3]	6677.9(9)	9093.7(6)
Z	4	4
ρ_{calc} [g cm^{-3}]	1.317	2.320
μ [mm^{-1}]	1.151	16.269
F(000)	2736.0	5792.0
Crystal size [mm^3]	0.2 × 0.18 × 0.16	0.24 × 0.16 × 0.15
Radiation	MoKα (λ = 0.71073)	MoKα (λ = 0.71073)
2Θ range for data collection [°]	4.092 to 58.058	3.808 to 53.998
Index ranges	-14 ≤ h ≤ 16, -34 ≤ k ≤ 27, -30 ≤ l ≤ 30	-32 ≤ h ≤ 32, -21 ≤ k ≤ 20, -29 ≤ l ≤ 29
Reflections collected	52712	91234
Independent reflections	8870 [R_{int} = 0.0363, R_{sigma} = 0.0298]	9928 [R_{int} = 0.0701, R_{sigma} = 0.0407]
Data/restraints/parameters	8870/1092/690	9928/36/443
Goodness-of-fit on F^2	1.080	1.071
Final R indexes [I>=2σ (I)]	R_1 = 0.0322, wR_2 = 0.0608	R_1 = 0.0323, wR_2 = 0.0707
Final R indexes [all data]	R_1 = 0.0514, wR_2 = 0.0713	R_1 = 0.0432, wR_2 = 0.0757
Largest diff. peak/hole [e Å^{-3}]	1.56/-0.93	3.25/-1.63

Table S 4 Crystal data and structure refinement of compounds **6** and **7**.

Compound	$Bi_4Sn_4H_2Tripp_8$ (**3**)	$Bi_2Sn_4Dipp_6$ (**7**)
CCDC number	1072051	1072052
Empirical formula	$C_{60}H_{93}Bi_2Sn_2$	$C_{76}H_{110}Bi_2O_2Sn_4$
Formula weight [g mol^{-1}]	1469.68	1948.35
Temperature [K]	100.01	100.0
Crystal system	triclinic	tetragonal
Space group	P-1	$P4_1$
a [Å]	14.1148(5)	14.1893(5)
b [Å]	14.1612(5)	14.1893(5)
c [Å]	31.9318(11)	37.5042(15)
a [°]	78.826(2)	90
β [°]	89.605(2)	90
γ [°]	81.323(2)	90
Volume [Å^3]	6188.3(4)	7551.0(6)
Z	4	4
ρ_{calc} [g cm^{-3}]	1.577	1.714
μ [mm^{-1}]	6.501	5.989
F(000)	2876.0	3792.0
Crystal size [mm^3]	0.28 × 0.25 × 0.09	0.28 × 0.24 × 0.21
Radiation	MoKα (λ = 0.71073)	MoKα (λ = 0.71073)
2Θ range for data collection [°]	1.3 to 54	2.172 to 54
Index ranges	-18 ≤ h ≤ 18, -18 ≤ k ≤ 18, -40 ≤ l ≤ 40	-18 ≤ h ≤ 18, -17 ≤ k ≤ 18, -47 ≤ l ≤ 43
Reflections collected	189677	192012
Independent reflections	26972 [R_{int} = 0.1346, R_{sigma} = 0.1027]	16239 [R_{int} = 0.0681, R_{sigma} = 0.0447]
Data/restraints/parameters	26972/403/1373	16239/469/782
Goodness-of-fit on F^2	1.134	1.064
Final R indexes [I>=2σ (I)]	R_1 = 0.0716, wR_2 = 0.1337	R_1 = 0.0509, wR_2 = 0.1147
Final R indexes [all data]	R_1 = 0.1222, wR_2 = 0.1534	R_1 = 0.0565, wR_2 = 0.1172
Largest diff. peak/hole [e Å^{-3}]	2.75/-2.50	3.59/-1.91
Flack parameter		-0.005(5)

Structure and details of the structure refinement for 1

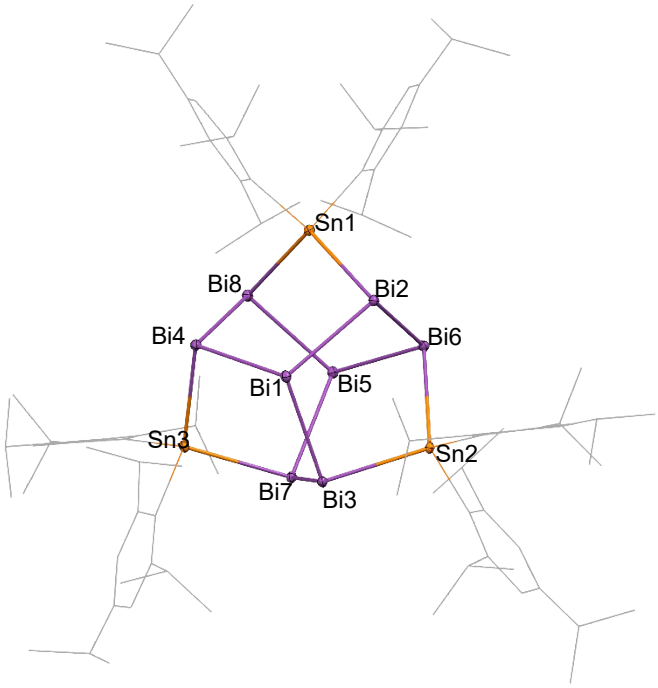

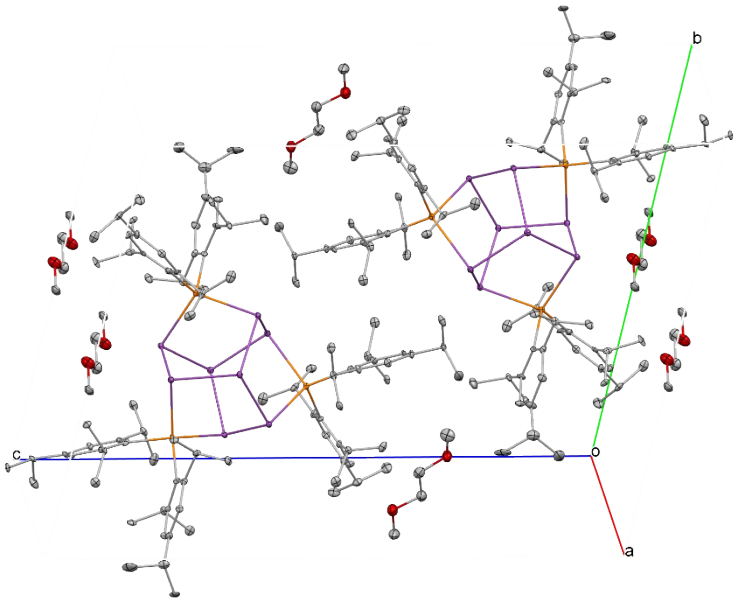

Figure S 29 Molecular structure and crystal packing of $Bi_8Sn_3Tripp_6$ (**1**). All non-carbons shown as 30% shaded ellipsoids. Hydrogens and solvent molecules are omitted for clarity. Selected bond lengths [Å] and angles [°] for **1**:Sn1-Bi2 2.9433(9), Sn1-Bi8 2.9034(8), Sn2-Bi3 2.9182(8), Sn2-Bi6 2.9094(9), Bi1-Bi2 3.0135(5), Bi1-Bi3 3.0188(7), Bi1-Bi4 3.0095(6), Bi2-Bi6 2.9399(6), Bi3-Bi7 2.9559(6), Bi4-Bi8 2.9470(5), Bi1-Bi2-Bi6 104.61(2), Bi1-Bi2-Sn1 100.29(2), Bi2-Sn1-Bi8 105.58(2), Bi3-Sn2-Bi6 107.94(3), C1-Sn1-C16 102.8(4), Bi2-Bi1-Bi3 105.19(2), Bi2-Bi1-Bi4 103.47(2), Bi3-Bi1-Bi4 103.94(2).

Structure and details of the structure refinement for 3

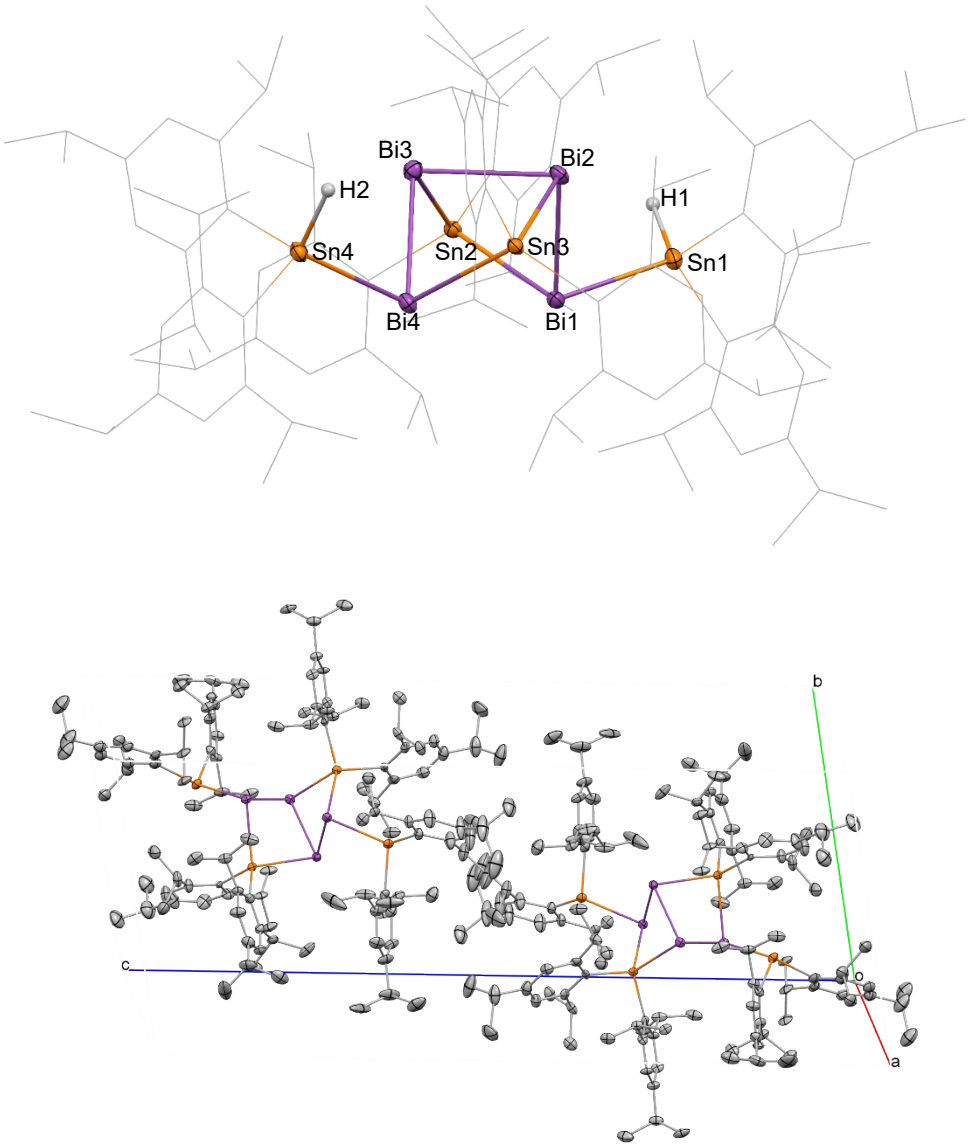

Figure S 30 Molecular structure and crystal packing of $Bi_4Sn_4H_2Tripp_8$ (**3**). All non-carbons shown as 30% shaded ellipsoids. Hydrogens except Sn-H are omitted for clarity. Selected bond lengths [Å] and angles [°] for **6**: Bi1-Bi2 2.9890(7), Bi1-Sn1 2.8812(9), Bi1-Sn2 2.9458(9), Bi2-Bi3 3.0293(7), Bi2-Sn3 2.9210(9), Sn1-H1 1.700, Bi1-Bi2-Bi3 85.00(2), Bi1-Bi2-Sn3 89.40(2), Bi1-Sn2-Bi3 87.90(3), Bi1-Sn1-H1 108.51, Bi2-Bi3-Bi4 86.39(2), Bi2-Sn3-Bi4 89.81(3), Bi2-Bi1-Sn1 88.68(1), Bi3-Bi4-Sn3 81.30(2), Bi4-Bi3-Sn2 91.10(2), Sn1-Bi1-Sn2 102.75(3), Sn3-Bi4-Sn4 99.05(3), C-Sn1-C 106(1), C-Sn2-C 105.5(4).

Structure and details of the structure refinement for 4

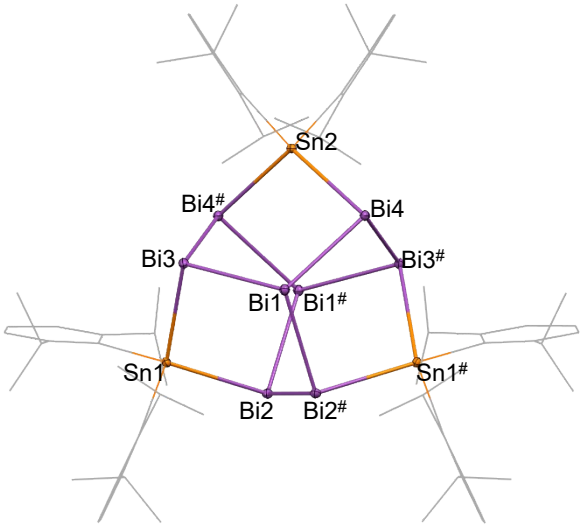

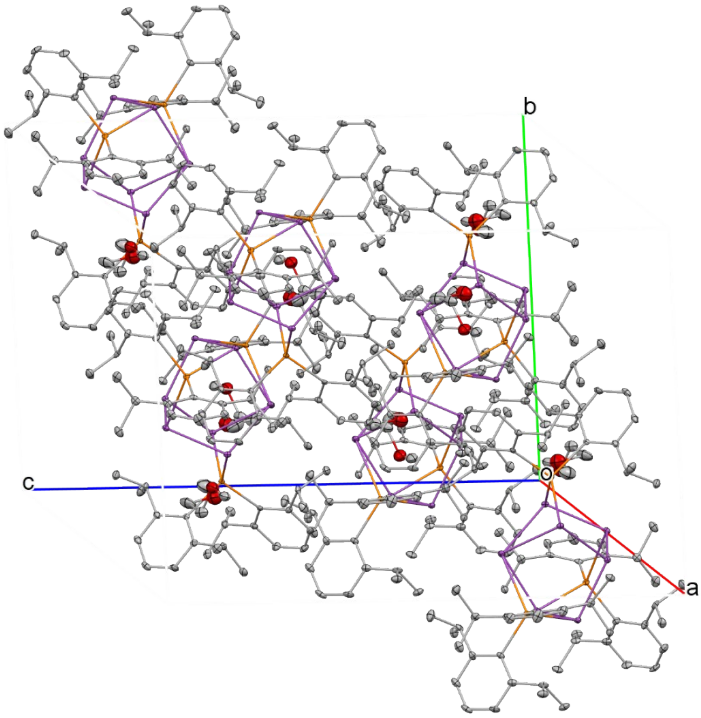

Figure S 31 Molecular structure and crystal packing of $Bi_8Sn_3Dipp_6$ (**4**). Selected bond lengths [Å] and angles [°] for **4**: Sn1-Bi2 2.9051(6), Sn1-Bi3# 2.9164(5), Sn2-Bi4 2.8965(4), Bi1-Bi2 2.9951(5), Bi1-Bi4 3.0136(4), Bi2-Bi2# 2.9714(5), Bi3-Bi4 2.9552(4), Bi2-Sn1-Bi3 106.471(2), Bi4-Sn2-Bi4# 107.41(2), C1-Sn1-C13 102.8(3), Bi2-Bi1-Bi4 102.74(2), Bi2-Bi1-Bi3# 103.79(2), Bi3#-Bi1-Bi4 105.17(2), Bi1-Bi2-Bi2# 104.70(2), Bi1-Bi4-Bi3 105.78(2), Bi1-Bi3#-Bi4# 103.85(2).

Structure and details of the structure refinement for 5

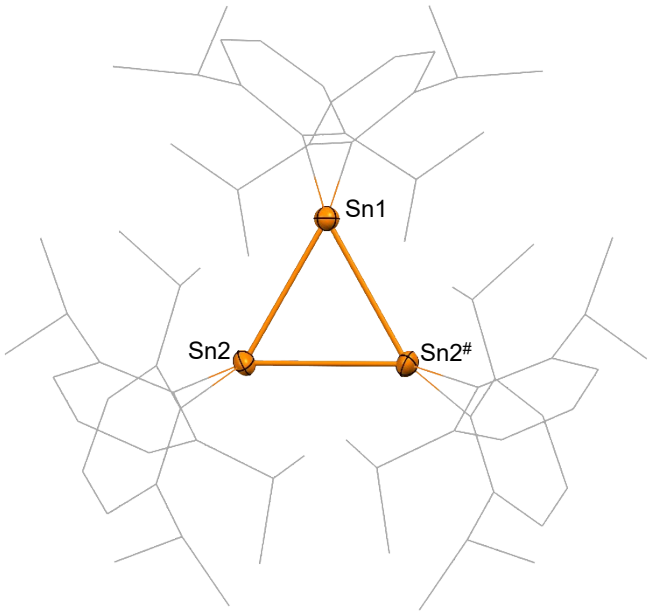

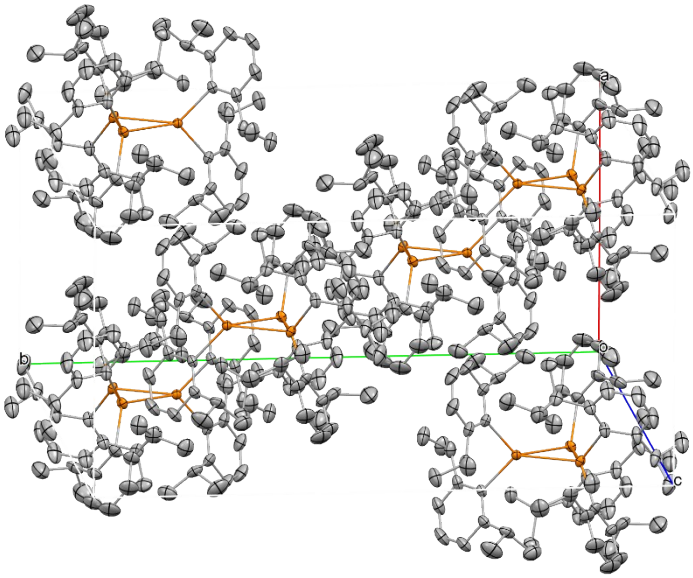

Figure S 32 Molecular structure of *cyclo*-$(Dipp_2Sn)_3$ (**5**). All non-carbons shown as 30% shaded ellipsoids. Hydrogens and solvent molecules are omitted for clarity. Selected bond lengths [Å] and angles [°] for **5**: Sn1-Sn2 2.9543(3), Sn2-Sn2# 2.8933(4), Sn1-Sn2-Sn2# 60.681(5), Sn2-Sn1-Sn2# 58.639(10), C1-Sn1-C1# 100.8(5), Sn13-Sn2-C25 103.4(4).

Structure and details of the structure refinement for 6

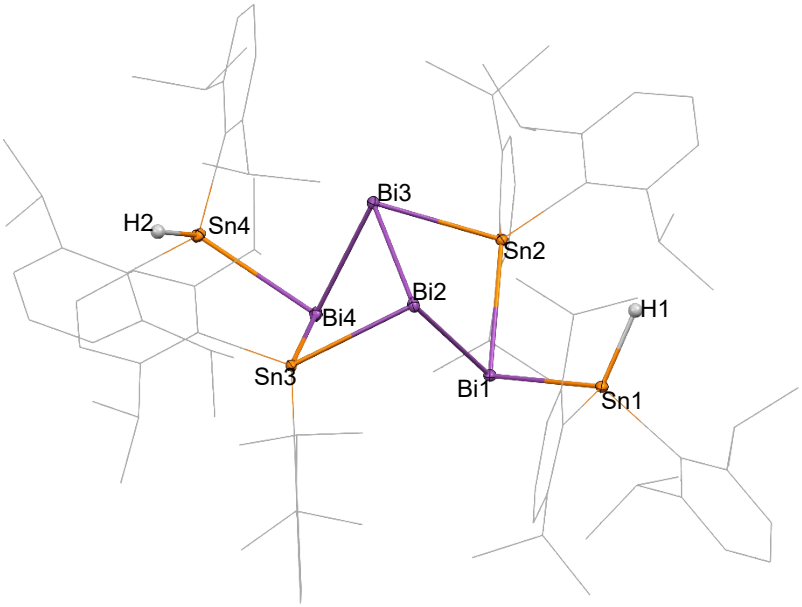

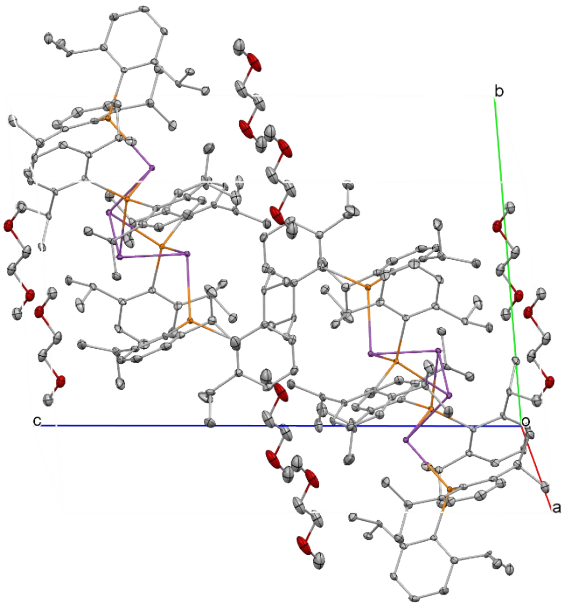

Figure S 33 Molecular structure and crystal packing of $Bi_4Sn_4H_2Dipp_8$ (**6**). All non-carbons shown as 30% shaded ellipsoids. Hydrogens except Sn-H and solvent molecules are omitted for clarity. Selected bond lengths [Å] and angles [°] for **3**: Bi1-Bi2 3.0027(5), Bi1-Sn1 2.8854(6), Bi1-Sn2 2.9213(6), Bi2-Bi3 3.0337(4), Bi2-Sn3 2.9223(7), Sn1-H1 1.66(7), Bi1-Bi2-Bi3 88.63(1), Bi1-Bi2-Sn3 90.06(1), Bi1-Sn2-Bi3 92.80(2), Bi1-Sn1-H1 109(2), Bi2-Bi3-Bi4 87.36(1), Bi2-Sn3-Bi4 90.65(2), Bi2-Bi1-Sn1 90.06(2), Bi3-Bi4-Sn3 81.01(1), Bi4-Bi3-Sn2 87.73(1), Sn1-Bi1-Sn2 102.45(2), Sn3-Bi4-Sn4 100.98(2), C-Sn1-C 102.5(3), C-Sn2-C 103.5(3).

Structure and details of the structure refinement for 7

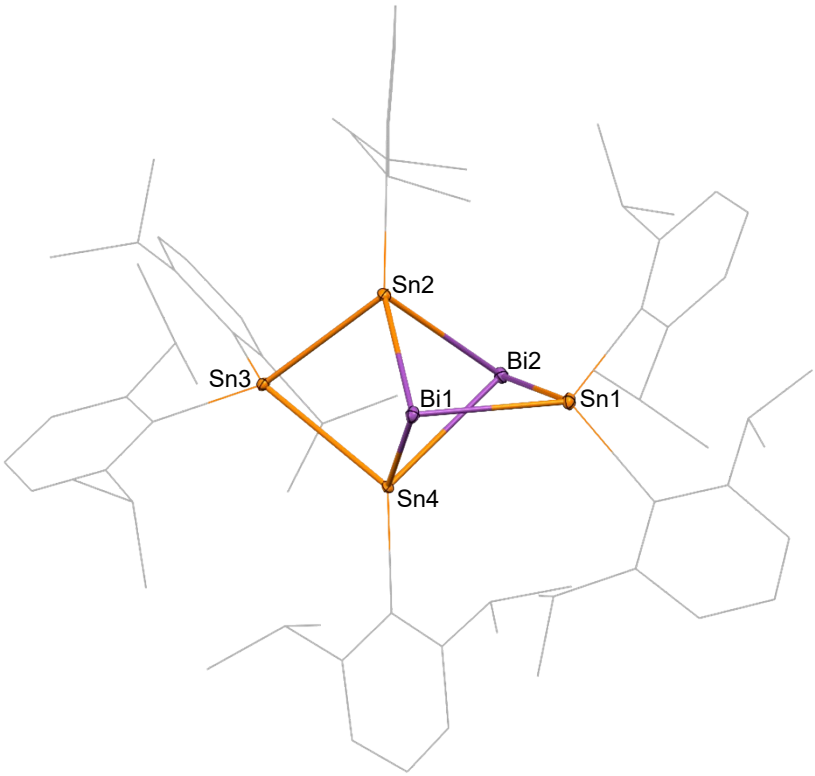

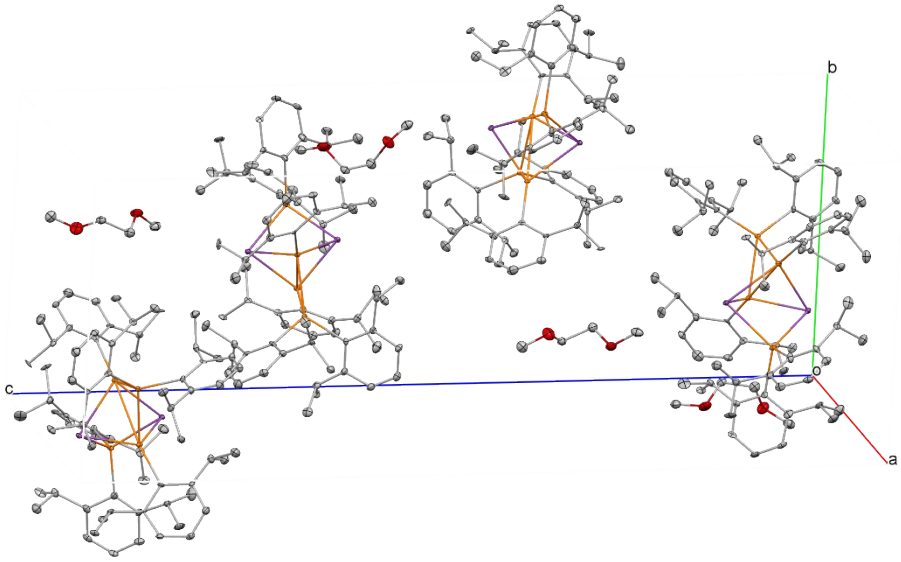

Figure S 34 Molecular structure of $Bi_2Sn_4Dipp_6$ (**7**). All non-carbons shown as 30% shaded ellipsoids. Hydrogens and solvent molecules are omitted for clarity. Selected bond lengths [Å] and angles [°] for **7**: Bi1···Bi2 4.083(1), Sn1-Bi1 2.916(1), Sn1-Bi2 2.909(1), Sn2-Bi1 2.954(1), Sn2-Bi2 2.964(1), Sn4-Bi1 2.969(1), Sn4-Bi2 2.937(1), Sn2-Sn3 2.831(1), Sn3-Sn4 2.828(1), Bi1-Sn1-Bi2 89.02(3), Bi1-Sn2-Bi2 87.26(3), Sn1-Bi1-Sn4 80.09(3), Sn2-Bi1-Sn4 69.13(3), Sn1-Bi2-Sn2 80.52(3), Bi1-Sn2-Sn3 91.43(4), Bi2-Sn2-Sn3 90.94(4), C1-Sn1-C13 100.9(7), C37-Sn3-C49 105.0(7), Sn2-Sn3-Sn4 72.84(4).

7 Quantum Chemical Investigations

All calculations have been carried out using the Gaussian09 program package[11] on a computing cluster with blade architecture. For geometry optimizations and the subsequent calculation of vibrational frequencies the mPW1PW91 hybrid functional[12] together with a Stuttgart-Dresden pseudopotential on tin and bismuth[13] and D95 all electron basis sets[14] on the remaining elements was used. For NBO analysis the all electron x2c-TZVPall basis[15] set was applied. Energies of selected canonical orbitals are provided in Table S 5.

Canonical orbitals visualized with GaussView (v5.0.9) are shown in the manuscript and in Figure S 34 to Figure S 36. Relevant NBOs for $Bi_8Sn_3Ph_6$, $Bi_4Sn_4H_2Ph_6$ are given in Tables S 6 and S7.

Table S8 summarizes structural parameters of all compounds in solid state obtained by X-Ray diffraction compared to calculated structural parameters for $Bi_8Sn_3Ph_6$, $Bi_4Sn_4H_2Ph_6$ and $Bi_2Sn_4Ph_6$.

Table S 5 Calculated HOMO, LUMO, HOMO-x as well as LUMO+x (x = 1-3) energies [eV] ([a.u.]) and energy difference ($E_{LUMO-HOMO}$) of $Bi_8Sn_3Ph_6$, $Bi_4Sn_4H_2Ph_8$ and $Bi_2Sn_4Ph_8$.

E	$Bi_8Sn_3Ph_6$	$Bi_4Sn_4H_2Ph_8$	$Bi_2Sn_4Ph_8$
LUMO+3	-1.61 (-0.05917)	-1.48 (-0.05439)	-1.19 (-0.04366)
LUMO+2	-1.94 (-0.07131)	-1.68 (-0.06173)	-1.24 (-0.04541)
LUMO+1	-2.28 (-0.08384)	-1.84 (-0.06747)	-1.55 (-0.05698)
LUMO	-2.29 (-0.08400)	-2.17 (-0.07986)	-1.61 (-0.05912)
HOMO	-5.47 (-0.20117)	-5.57 (-0.20454)	-5.36 (-0.19706)
HOMO-1	-5.82 (-0.21392)	-5.78 (-0.21239)	-6.14 (-0.22573)
HOMO-2	-5.83 (-0.21418)	-6.33 (-0.23247)	-6.29 (-0.23101)
HOMO-3	-6.06 (-0.22278)	-6.43 (-0.23631)	-6.43 (-0.23632)
$\Delta E_{HOMO-LUMO}$	3.19 (0.117177)	3.39 (0.12468)	3.75 (0.13794)

NBO analysis

$Bi_8Sn_3Ph_6$

Electron density of σ bond (Bi-Bi) orbitals donate into σ* bond orbitals of other/adjacent Bi-Bi bonds and Sn-C bonds. Yet, occupation/population of the σ* orbitals involving apical Bi atoms (Bi1, Bi5 for **1**; Bi1 and Bi1# for **4**) is twice as high (0.084 e^-) as σ* bond orbitals of Bi^{eq}-Bi^{eq}.

$Bi_4Sn_4H_2Ph_8$

Electron density of σ bonding orbitals of Bi1-Bi2 and Bi4-Bi5, respectively, donate electron density into σ* orbitals of Bi2-Bi3. Also back donation is observed, which, however, turns out to be somewhat lower. Accordingly, these donations result in a higher occupation of (antibonding) σ* orbitals of Bi2-Bi3 (0.024 e^-) than for Bi1-Bi2 and Bi4-Bi5, respectively (0.014 e^-).

Table S 6 Selected NBOs for $Bi_8Sn_3Ph_6$

Orbital No.	lone pair at Bi	Occupancy [e^-] and character	Orbital No.		Occupancy [e^-] and character
103	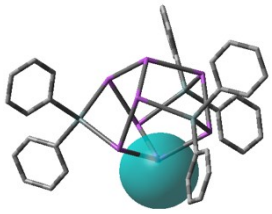	1.940 lone pair, Bi5			
104	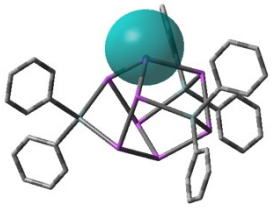	1.940 lone pair, Bi1			
105	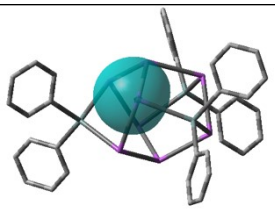	1.920 lone pair, Bi4			
106	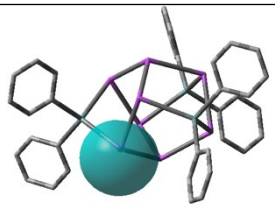	1.921 lone pair, Bi8			
107	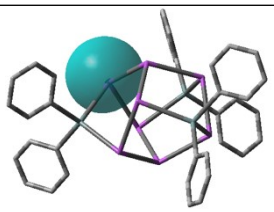	1.920 lone pair, Bi3			
108	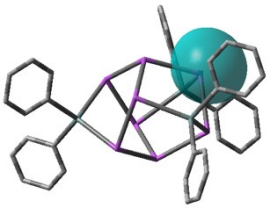	1.921 lone pair, Bi2			
109	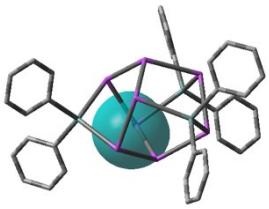	1.921 lone pair, Bi7			

110	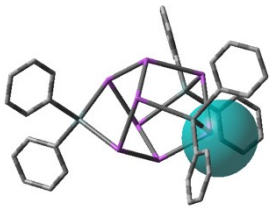	1.920 lone pair, Bi6			
	Bi-Bi σ-orbitals			Bi-Bi σ^*-orbitals	
117	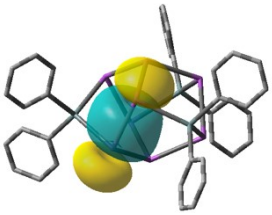	σBi3-Bi7 1.945	156	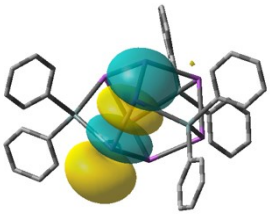	σ^*Bi3-Bi7 0.049
118	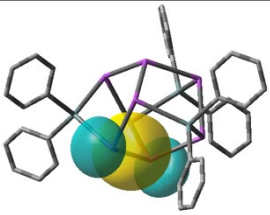	σBi5-Bi8 1.955	150	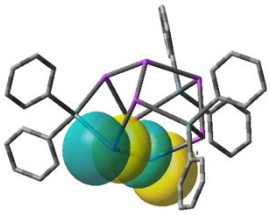	σ^*Bi5-Bi8 0.084
119	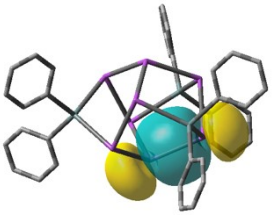	σBi5-Bi6 1.955	155	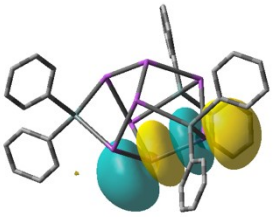	σ^*Bi5-Bi6 0.084
120	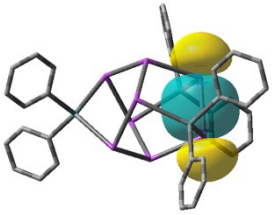	σBi2-Bi6 1.944	158	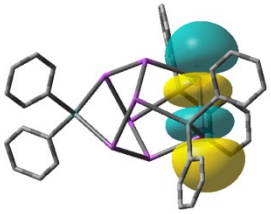	σ^*Bi2-Bi6 0.047
121	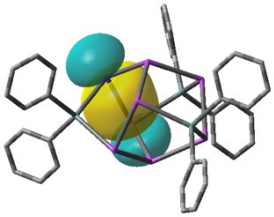	σBi4-Bi8 1.944	157	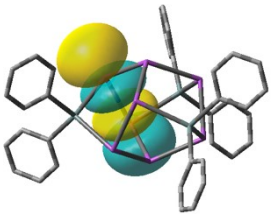	σ^*Bi4-Bi8 0.047
124	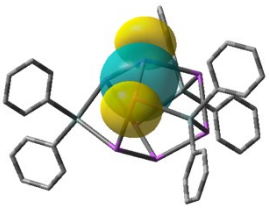	σBi1-Bi3 1.954	151	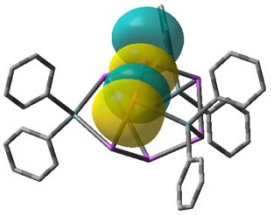	σ^*Bi1-Bi3 0.084

125	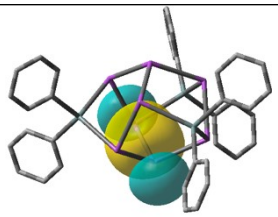	σBi5-Bi7 1.955	153	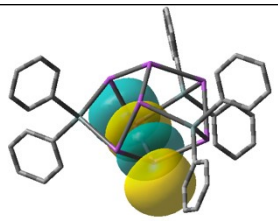	σ*Bi5-Bi7 0.084
126	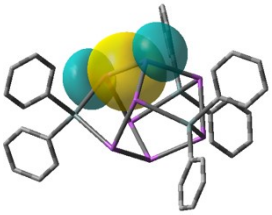	σBi1-Bi4 1.954	154	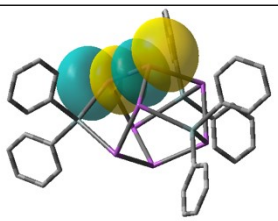	σ*Bi1-Bi4 0.084
127	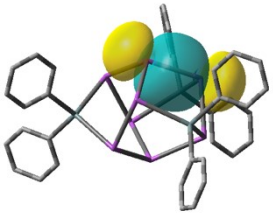	σBi1-Bi2 1.954	152	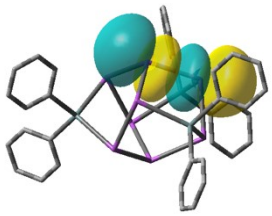	σ*Bi1-Bi2 0.085

Table S 7 Selected NBOs for $Bi_4Sn_4Ph_6H_2$

Orbital No.	lone pair at Bi	Occupancy [e$^-$] and character	Orbital No.		Occupancy [e$^-$] and character
90	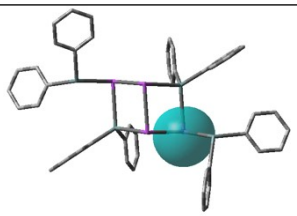	1.948 lone pair, Bi4			
91	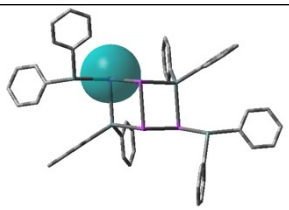	1.949 lone pair, Bi1			
92	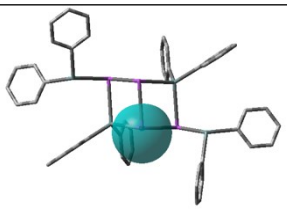	1.965 lone pair, Bi3			
93	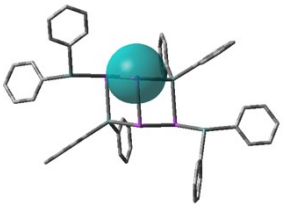	1.967 lone pair, Bi2			
	Bi-Bi σ-orbitals			Bi-Bi σ^*-orbitals	
87	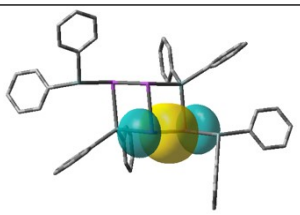	σBi3-Bi4 1.947	184	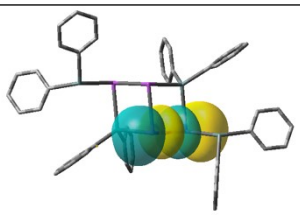	σ^*Bi3-Bi4 0.014
88	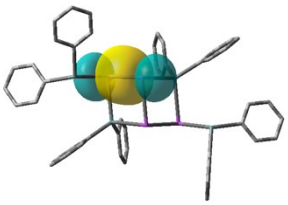	σBi1-Bi2 1.948	185	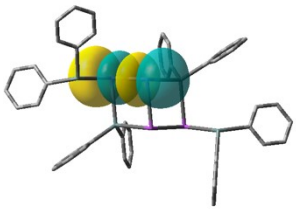	σ^*Bi1-Bi2 0.014
89	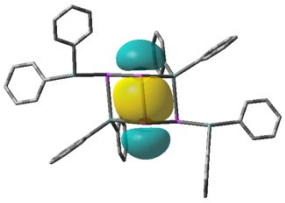	σBi2-Bi3 1.955	210	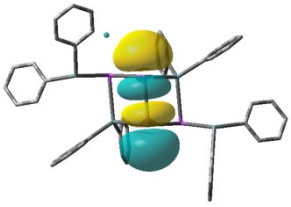	σ^*Bi2-Bi3 0.024

Table S 8 Summary of calculated structural parameters for $Bi_8Sn_3Ph_6$, $Bi_4Sn_4H_2Ph_6$ and $Bi_2Sn_4Ph_6$ compared to structural parameter in solid state structures.

Compound	**Bi^{apical}-Bi^{equ} [Å]**		**Bi^{equ}-Bi^{equ} [Å]**		**Bi-Sn [Å]**	
	exp	**Calc**	**exp**	**calc**	**exp**	**calc**
$Bi_8Sn_3Tripp_6$ (**1**)	Bi1-Bi2 3.0135(5) Bi1-Bi3 3.0188(7) Bi1-Bi4 3.0095(6)		Bi2 Bi6 2.9399(6) Bi3 Bi7 2.9559(6) Bi4 Bi8 2.9470(5)		Bi2-Sn1 2.9433(9) Bi8-Sn1 2.9034(8) Bi3-Sn2 2.9182(8), Bi6-Sn2 2.9094(9) Bi4-Sn3 2.9197(9) Bi7-Sn3 2.9027(9)	
		3.023 3.022 3.024		2.982 2.982 2.981		2.923 2.921 2.922 2.922
$Bi_8Sn_3Dipp_6$ (**4**)	Bi1-Bi2 2.9951(5) Bi1-Bi3 3.0053(4) Bi1-Bi4 3.0136(4)		Bi2-Bi2# 2.9714(5) Bi3-Bi4 2.9552(4) Bi3#-Bi4# 2.9552(4)		Bi2-Sn1 2.9051(6) Bi3#-Sn1 2.9164(5) Bi4-Sn2 2.8965(4)	

	Bi-Bi [Å]				**Bi-Sn [Å]**	
	exp	calc	exp	calc	exp	calc
$Bi_4Sn_4H_2Tripp_8$ (**3**)	Bi1-Bi2 2.9890(7) Bi3-Bi4 3.0129(6)		Bi2-Bi3 3.0293(7)		Bi1-Sn1 2.8812(9) Bi1-Sn2 2.9458(9) Bi2-Sn3 2.9210(9) Bi4-Sn4 2.879(1)	
		3.050 3.056		3.078		2.918 2.941 2.938 2.915
$Bi_4Sn_4H_2Dipp_8$ (**6**)	Bi1-Bi2 3.0027(5) Bi3-Bi4 2.9890(6)		Bi2-Bi3 3.0337(4)		Bi1-Sn1 2.8854(6) Bi1-Sn2 2.9213(6) Bi2-Sn3 2.9223(7) Bi4-Sn4 2.8923(5)	

	Bi···Bi [Å]		**Bi-Sn [Å]**	
	exp	**calc**	**exp**	**calc**

$Bi_2Sn_4Dipp_6$ (**7**)	Bi1···Bi2 4.083(1)	4.194	Bi1-Sn1 2.916(1) Bi2-Sn1 2.954(1) Bi1-Sn4 2.969(1)	2.944 2.991 3.000

Canonical orbitals for valence MOs

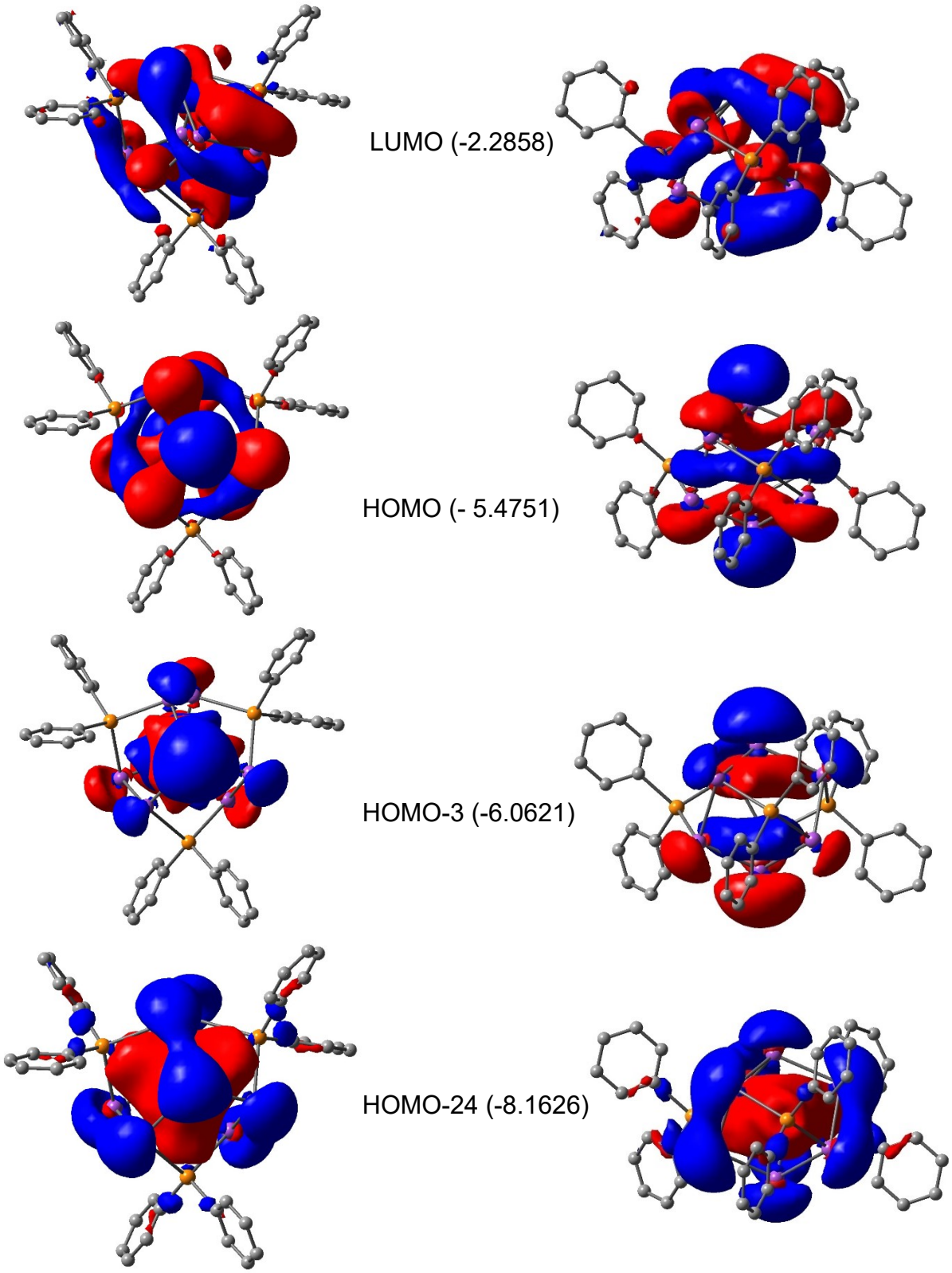

Figure S 35 Canonical valence molecular orbitals and orbital energies [eV] for $Bi_8Sn_3Ph_6$. Sn, Bi and C atoms shown as orange, purple and grey balls, respectively.

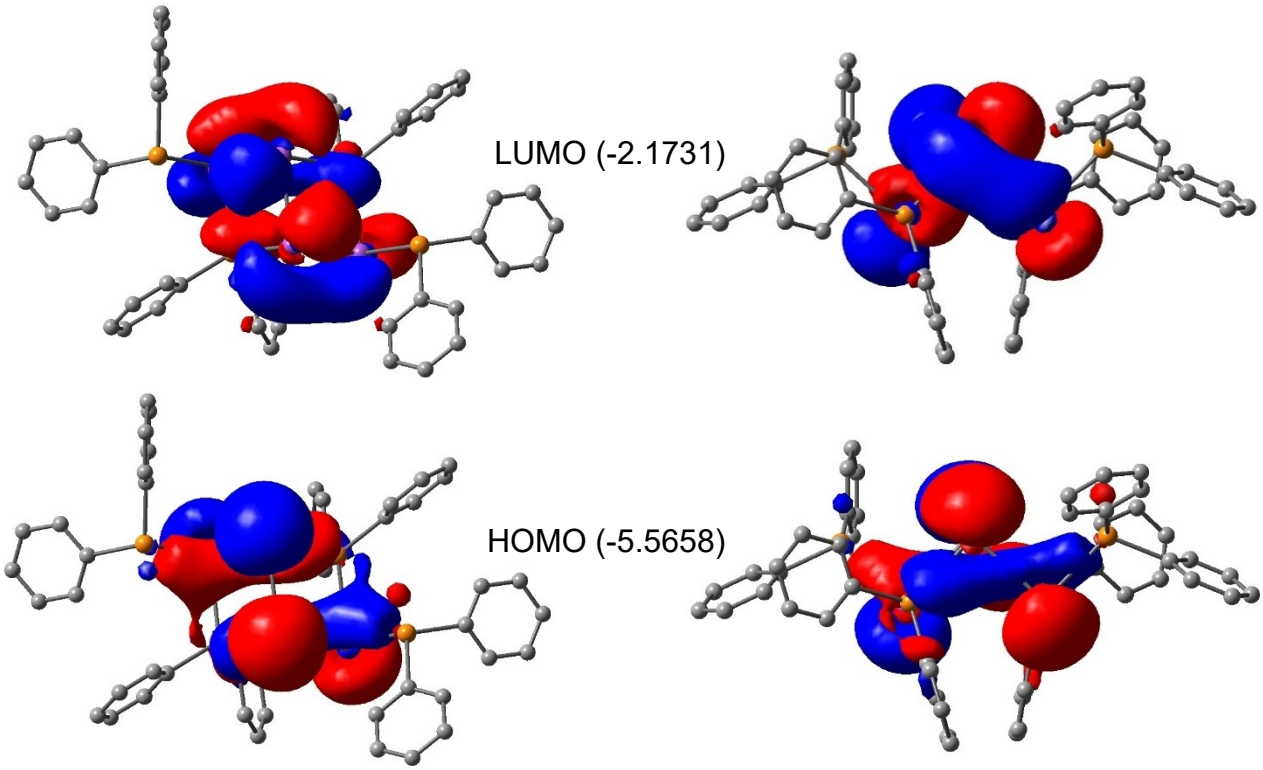

Figure S 36 Canonical valence molecular orbitals and orbital energies [eV] for $Bi_4Sn_4Ph_8$. Sn, Bi and C atoms shown as orange, purple and grey balls, respectively.

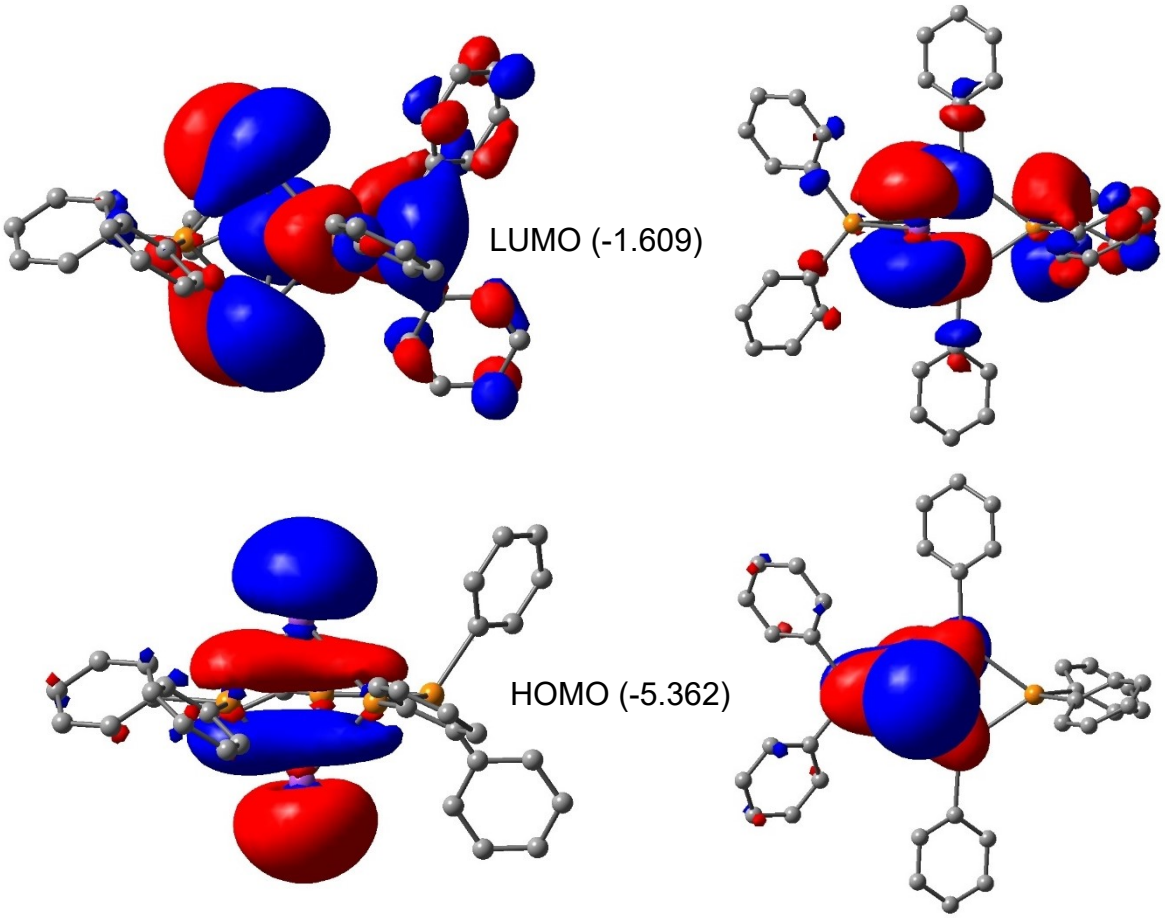

Figure S 37 Canonical valence molecular orbitals and orbital energies [eV] for $Bi_2Sn_4Ph_6$. Sn, Bi and C atoms shown as orange, purple and grey balls, respectively.

9 References

[1] B. G. Steller, R. C. Fischer, *Eur. J. Inorg. Chem.* **2019**, *2019*, 2591–2597.

[2] M. J. S. Gynane, A. Hudson, M. F. Lappert, P. P. Power, *Dalton Trans* **1980**, 2428–2433.

[3] S. Masamune, L. R. Sita, *J. Am. Chem. Soc.* **1985**, *107*, 6390–6391.

[4] R. H. Blessing, *Acta Cryst. A* **1995**, *A51*, 33–38.

[5] G. M. Sheldrick, *SADABS Version 2.10 Siemens Area Detector Correction.*, Universität Göttingen, Göttingen, Germany, **2003**.

[6] G. M. Sheldrick, *SHELXTL Version 6.1. Bruker AXS, Inc.*, Madison, WI, **2002**.

[7] G. M. Sheldrick, *GM SHELXS97 and SHELXL97*, Universität Göttingen, Göttingen, Germany, **2002**.

[8] O. V. Dolomanov, L. J. Bourhis, R. J. Gildea, J. A. K. Howard, H. Puschmann, *J. Appl. Cryst.* **2009**, *42*, 339–341.

[9] A. L. Spek, *J. Appl. Cryst.* **2003**, *36*, 7–13.

[10] A. L. Spek, *Acta Cryst. D* **2009**, *65*, 148–155.

[11] M. J. Frisch, G. W. Trucks, H. B. Schlegel, G. E. Scuseria, M. A. Robb, J. R. Cheeseman, G. Scalmani, V. Barone, B. Mennucci, G. A. Petersson, H. Nakatsuji, M. Caricato, X. Li, H. P. Hratchian, A. F. Izmaylov, J. Bloino, G. Zheng, J. L. Sonnenberg, M. Hada, M. Ehara, K. Toyota, R. Fukuda, J. Hasegawa, M. Ishida, T. Nakajima, Y. Honda, O. Kitao, H. Nakai, T. Vreven, J. A. Montgomery, Jr., J. E. Peralta, F. Ogliaro, M. Bearpark, J. J. Heyd, E. Brothers, K. N. Kudin, V. N. Staroverov, T. Keith, R. Kobayashi, J. Normand, K. Raghavachari, A. Rendell, J. C. Burant, S. S. Iyengar, J. Tomasi, M. Cossi, N. Rega, J. M. Millam, M. Klene, J. E. Knox, J. B. Cross, V. Bakken, C. Adamo, J. Jaramillo, R. Gomperts, R. E. Stratmann, O. Yazyev, A. J. Austin, R. Cammi, C. Pomelli, J. W. Ochterski, R. L. Martin, K. Morokuma, V. G. Zakrzewski, G. A. Voth, P. Salvador, J. J. Dannenberg, S. Dapprich, A. D. Daniels, O. Farkas, J. B. Foresman, J. V. Ortiz, J. Cioslowski, and D. J. Fox, *Gaussian Inc*, Wallingford CT, **2013**.

[12] C. Adama, V. Barone, *J. Chem. Phys.* **1998**, *108*, 664–675.

[13] A. Bergner, M. Dolg, W. Küchle, H. Stoll, H. Preuß, *Mol. Phys.* **1993**, *80*, 1431–1441.

[14] T. H. Dunning Jr, P. J. Hay, in *Modern Theoretical Chemistry* (Ed.: H.F. Schaefer), Plenum, New York, **1977**, pp. 1–28.

[15] P. Pollak, F. Weigend, *J. Chem. Theory Comput.* **2017**, *13*, 3696–3705.